

Thermodynamic and Structure–Property Study of Liquid–Vapor Equilibrium for Aroma Compounds

ANNE TROMELIN,^{*,†} ISABELLE ANDRIOT,[†] MIRELA KOPJAR,^{†,§} AND ELISABETH GUICHARD[†]

[†]Centre des Sciences du Goût et de l'Alimentation, UMR1324 INRA, UMR6265 CNRS Université de Bourgogne, Agrosup Dijon, F-21000 Dijon, and [§]Faculty of Food Technology, F. Kuhaca 18, HR-31000 Osijek, Croatia

Thermodynamic parameters (T , ΔH° , ΔS° , K) were collected from the literature and/or calculated for five esters, four ketones, two aldehydes, and three alcohols, pure compounds and compounds in aqueous solution. Examination of correlations between these parameters and the range values of ΔH° and ΔS° puts forward the key roles of enthalpy for vaporization of pure compounds and of entropy in liquid–vapor equilibrium of compounds in aqueous solution. A structure–property relationship (SPR) study was performed using molecular descriptors on aroma compounds to better understand their vaporization behavior. In addition to the role of polarity for vapor–liquid equilibrium of compounds in aqueous solution, the structure–property study points out the role of chain length and branching, illustrated by the correlation between the connectivity index CHI-V-1 and the difference between T and $\log K$ for vaporization of pure compounds and compounds in aqueous solution. Moreover, examination of the esters' enthalpy values allowed a probable conformation adopted by ethyl octanoate in aqueous solution to be proposed.

KEYWORDS: Aroma compounds; retention–release equilibrium; thermodynamic values; hydrophobic effect; structure–property relationships; molecular descriptors

INTRODUCTION

Flavor perception is one of the main attributes that govern acceptability of foods by consumers. To be perceived, aroma compounds have first to be released from the food matrix into the vapor phase and then reach the olfactory receptors. During food consumption, the release of aroma compounds is governed by the interactions of these small molecules with food constituents, such as proteins, polysides, and lipids (1). Proteins, for example, interact with aroma compounds mostly by hydrophobic binding, as was demonstrated for homologous series of alcohols, esters, and ketones (2, 3). Aroma compounds, which have a high affinity for proteins, are thus less released in the vapor phase and also less perceived in the presence of proteins than in water (4). Due to the hydrophobic properties of most of the aroma compounds, the most important factor influencing gas/matrix partitioning is the presence of lipids. Taking the vapor pressure of aroma compounds and their gas/water and gas/oil partition coefficients into account, it is then possible to predict the gas/emulsion partition coefficients (5). The calculated partition coefficients were found to be in good agreement with experimental data obtained either in model emulsions or in custard desserts (6, 7). However, the gas/water partition coefficients are not available in the literature for a great number of aroma compounds and, when available, the data are often not comparable due to the different methodologies and different temperatures used for the experiment. A compilation of literature data obtained for gas/water partition

coefficients of three esters at different temperatures was done, after conversion into the same unit (8), and then used to first predict gas/water partition coefficients at temperatures other than those used in experiments in order to calculate retention of these aroma compounds in different matrices. Most studies focus on homologous series of compounds and highlight the role of hydrophobicity. When a large range of chemical classes was considered, it was suggested that not only hydrogen and hydrophobic bonds between molecules but also the geometry of the molecule may influence its thermodynamic properties such as its volatility (9) or its affinity for a given protein (10). There is thus a need to take molecular descriptors other than the classical $\log P$ value into account to try to better understand the partition of aroma compounds between water and air and then the variations of this coefficient as a function of the composition of the medium. In this way, we investigated the relationships between chemical structure and thermodynamic properties using molecular descriptors provided by the commercially available QSAR⁺ Cerius² package (Accelrys Inc.).

Quantitative structure–activity relationships (QSAR) methods attempt to find relationships between the properties of molecules and an experimental response; the assumption is that changes in molecular properties elicit different responses (11, 12). The QSAR study is intended to represent a physicochemical property in a simple mathematical relationship, the QSAR equation: $ER = f(p_1, p_2, p_3, \dots, p_n)$, where ER are the calculated thermodynamic values of equilibrium and p_i the molecular descriptor values. A molecular descriptor is a numerical value that encodes a molecular property by a symbolic representation (13). These approaches were

*Author to whom correspondence should be addressed (e-mail Anne.Tromelin@dijon.inra.fr; telephone 33380693512; fax 33380693227).

already applied with success on gas/product partition coefficients of aroma compounds in different model matrices. For example, in saline solutions and carrageenan gels, a QSPR approach explained the retention of 12 aroma compounds (esters and ketones) by molecular descriptors related to electronic properties of charge repartition on the molecule and molecule shapes (14). In another study on model dairy gels, the surface-weighted negatively charged partial surface area seemed to play a critical role in the behavior of aroma compounds (15).

In the present study, our purpose was to investigate the nature of involved interactions between liquid medium and aroma compounds. Therefore, we tried to identify the most important molecular property involved in the thermodynamic vaporization property for a training set of several aroma compounds. In this way, we first collected data on several aroma compounds from different chemical classes, previously studied in the context of the CANAL-ARLE project (16), for pure compounds and compounds in aqueous solution. Second, we voluntarily limited our scope to linear monovariate regressions and identified simple linear correlations between molecular descriptors and thermodynamic values. Our present goal was not to generate predictive models but to propose a qualitative interpretation of these correlations to better understand the behavior of the current set of aroma compounds as pure compound or diluted in water (17).

MATERIALS AND METHODS

Material. The physicochemical properties of the 14 selected aroma compounds are given in **Table 1**.

Thermodynamic Standard Value Calculation. Thermodynamic standard values in aqueous solution were calculated according to the following procedure.

Determination of Gas/Water Partition Coefficient. The gas/water partition coefficient (PC) describes the distribution of volatile compounds between the water and the gas phase (eq 1)

$$PC = \frac{C_{\text{vap}}}{C_{\text{liq}}} \quad (1)$$

with C_{vap} the concentration of the volatile compound in the headspace and C_{liq} the concentration of the volatile compound in water (C_{vap} and C_{liq} are expressed in mol L^{-1}).

The determination of gas/water partition coefficients of different aroma compounds was conducted in different laboratories, which were all partners within the framework of the CANAL-ARLE project, by the phase ratio variation (PRV) method (18). This method is based on the influence of the sample volume on the concentration of volatile in the headspace, which leads to eq 2

$$\frac{1}{A} = \frac{1}{f_i \times C_{\text{liq}}} \times (PC + \beta) \quad (2)$$

where A (au) is the chromatographic peak area at equilibrium, f_i is the specific substance-response factor detector, which depends on both the particular system and the analytical conditions, C_{liq} is the sample concentration in water (assumed to be equal to initial concentration), and β is the ratio $V_{\text{vap}}/V_{\text{liq}}$. Variables in this equation are the phase ratio (β) and the peak area (A). Thus, eq 2 corresponds to a linear equation of the following type (eq 3):

$$1/A = a + b\beta \quad (3)$$

$PC = a/b$ is calculated from the values of a and b obtained by plotting $1/A$ against β in the linear zone.

Standardization of Gas/Water Partition Coefficients from the Literature. All of the data from the literature were thus converted into molar concentration to be compared with data from the CANAL-ARLE project, which were expressed in that unit according to the previously used calculation (8).

Calculation of Equilibrium Thermodynamic Standard Values. For equilibrium, the vant'Hoff's law links the equilibrium constant to the temperature according to eq 4

$$\frac{d \ln K}{dT} = \frac{\Delta H^\circ}{RT^2} \quad (4)$$

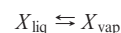
where K is the equilibrium constant, ΔH° is the enthalpy of the chemical or physicochemical reaction (expressed in J mol^{-1}), R is the universal gas constant ($R = 8.314 \text{ J K}^{-1} \text{ mol}^{-1}$), and T is the temperature (expressed in Kelvin).

Assuming that ΔH° remains constant for the considered temperature range (Ellingham approximation), the previous equation should be integrated as follows (eq 5):

$$\ln K = -\frac{\Delta H^\circ}{RT} + C \quad (5)$$

If the equilibrium constant values are known at different temperatures, it is possible to perform a linear regression calculation of $\ln(K)$ versus $1/T$.

The use of a thermodynamic equilibrium constant is required for the regression calculation. The equilibrium constant K of a compound (X) at equilibrium between a liquid phase and a gas phase



is the ratio of the activities $a(X)$ of the compound in each phase (eq 6):

$$K = \frac{a(X)_{\text{vap}}}{a(X)_{\text{liq}}} \quad (6)$$

Assuming that the vapor phase obeys the Boyle–Mariotte law and that the liquid phase should be considered as a diluted solution, $a(X)_{\text{vap}} = p_X/P^\circ$ and $a(X)_{\text{liq}} = C_{\text{liq}}/C_0$, we can write

$$K = \frac{p_X/P^\circ}{C_{\text{liq}}/C_0} \quad (7)$$

where C_{liq} is the concentration of the compound (X) in the liquid phase (mol L^{-1}), C_0 is the reference concentration ($C_0 = 1 \text{ mol L}^{-1}$), p_X is the partial pressure of the compound (X) in the vapor phase (atm), and P° is the reference pressure ($P^\circ = 1 \text{ atm}$).

According to $p_X V = n_X RT$ (true if vapor phase volume is constant), we can write

$$p_X = \frac{n_{X,\text{vap}}}{V_{\text{vap}}} \times RT = C_{\text{vap}} \times RT \quad (8)$$

with $R = 0.0821 \text{ L atm K}^{-1} \text{ mol}^{-1}$, T in K, and p_X in atm, and in this way, we obtain eq 9:

$$K = \frac{C_{\text{vap}}}{C_{\text{liq}}} \times RT = PC \times RT \quad (9)$$

Knowing the linear relationship regression parameters (slope and intercept) of $\ln K$ versus $1/T$ and according to the following relationship between K , ΔG° , ΔH° , and ΔS° at equilibrium (eq 10)

$$\Delta G^\circ(T_{\text{eq}}) = -RT_{\text{eq}} \ln K(T_{\text{eq}}) = \Delta H^\circ - T_{\text{eq}} \Delta S^\circ = 0 \quad (10)$$

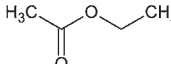
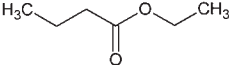
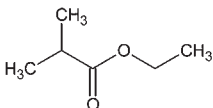
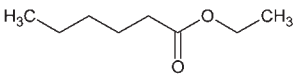
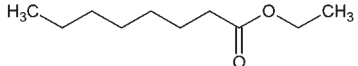
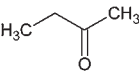
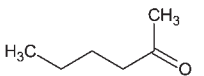
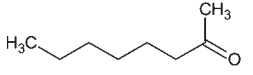
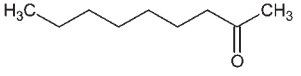
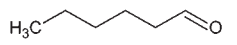
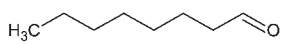

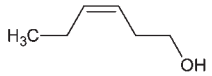
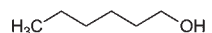
it is possible to calculate K values at any temperature (in a range smaller than 100°C), T_{eq} , the temperature to which the equilibrium displacement is reversed, ΔH° value ($\Delta H^\circ = \text{slope} \times R$), and ΔS° value ($\Delta S^\circ = \Delta H^\circ / RT_{\text{eq}}$).

For pure compounds, we used available literature data (<http://webbook.nist.gov/chemistry/>) of T_{vap} and $\Delta H^\circ_{\text{vap}}$ values to calculate $\Delta S^\circ_{\text{vap}}$ and $K(T)$ values.

We selected the temperature 30°C (303 K) for K calculations for both pure aroma compounds and aroma compounds solved in water. For the structure–activity study, we used $1/K$ values, which correspond to shift to liquid phase; $1/K$ values are called K_{liq} for pure aroma compounds and K_{ret} for aroma compounds in aqueous solution.

Chemistry: Structure–Property Study. The three-dimensional molecular structures of the 14 aroma compounds were calculated using DS

Table 1. Main Physicochemical Characteristics of Aroma Compounds

N°	Name	n°CAS	MW (g mol ⁻¹)	Molecular Formula	Structure	T _{vap} (K) ^a	ΔH ⁰ _{vap} (kJ mol ⁻¹)
1	ethyl acetate	141-78-6	88	C ₄ H ₈ O ₂		350	35.0 ^a
2	ethyl butanoate	105-54-4	116	C ₆ H ₁₂ O ₂		394	42.0 ^a
3	ethyl 2-methylpropanoate	97-62-1	116	C ₆ H ₁₂ O ₂		383	35.6 ^a
4	ethyl hexanoate	123-66-0	144	C ₈ H ₁₆ O ₂		440	52.0 ^a
5	ethyl octanoate	106-32-1	172	C ₁₀ H ₂₀ O ₂		480	59.0 ^a
6	butan-2-one	78-93-3	72	C ₄ H ₈ O		353	35.0 ^a
7	hexan-2-one	591-78-6	100	C ₆ H ₁₂ O		400	43.0 ^a
8	octan-2-one	111-13-7	128	C ₈ H ₁₆ O		446	39.8 ^a
9	nonan-2-one	821-55-6	142	C ₉ H ₁₈ O		468	56.4 ^a
10	hexanal	66-25-1	100	C ₆ H ₁₂ O		402 ^b	45.3 ^b
11	octanal	124-13-0	128	C ₈ H ₁₆ O		444	43.0 ^a
12	butan-1-ol	71-36-3	74	C ₄ H ₁₀ O		391	51.0 ^a
13	(3Z)-hex-3-en-1-ol (cis-3-hexenol)	928-96-1	100	C ₆ H ₁₂ O		429	57.7 ^a
14	hexan-1-ol	111-27-3	107	C ₆ H ₁₄ O		430	61.0 ^a

^a Available values on National Institute of Standard and Technology (NIST) Chemistry WebBook (<http://webbook.nist.gov/chemistry/>).

Viewer Pro 6.0 (Accelrys Inc., San Diego, CA). Minimization was then carried out using Dreiding Forcefield available in Discovery Studio package (number of iterations = 5000, convergence criterion = 0.0001 kcal mol⁻¹).

Ethyl octanoate conformers were generated using Catalyst/COMPARE (Catalyst version 4.9.1 software; Accelrys Inc., August 2004) running on a Silicon Graphics workstation (SGI-O₂), and the "best conformer generation" was applied to provide the best conformational coverage for a maximum number of conformers generated of 250 in a 0–20 kcal mol⁻¹ range from the global minimum energy (19, 20).

The molecules were exported to Cerius² and then analyzed with Cerius² software (version 4.11; Accelrys Inc., 2006) running on a Pentium IV computer with the Linux Red Hat Enterprise 2.1 OS. The modules QSAR⁺ and Descriptors⁺ were used for generating the descriptor collec-

tion and simple linear regressions. In the present work, we retained 54 descriptors belonging to the classical groups of descriptors (electronic, spatial, structural, thermodynamic, and topological descriptors), the values of which do not depend on the orientation.

In this study, we considered simple linear correlations between thermodynamic values and molecular descriptor values. Although our purpose was not to derive predictive QSAR models, validation procedures were carried out to verify that the equations possess a reliable internal predictive power and were not obtained by chance (21, 22). Therefore, we used validation tools available in the Cerius² package (r^2 , F test, $CV-r^2$, bootstrap- r^2 , and Y randomization at 99% confidence level).

The cross-validation process repeats the regression many times on subsets of data. Usually each molecule is left out in turn, and the r^2 is

Table 2. Temperature Data, Regression Parameters (r^2 and F Test), and Calculated Equilibrium Thermodynamic Standard Values T_{eq} and $\Delta H_{\text{eq}}^\circ$ for Aroma Compounds in Aqueous Solution

no.	name	T ($^\circ\text{C}$)	no. of obs/ F_{crit}	exptl lnK vs $1/T$		calcd lnK vs exptl ln K		T_{eq}^a (K)	$\Delta H_{\text{eq}}^\circ$ (kJ mol^{-1})
				r^2	F test	r^2	F test		
1	ethyl acetate (23–25, 49, 50–68)	0, 4, 10, 20, 25, 28, 30, 37, 40, 50, 60, 70, 80	21/4.4	0.99	1196.0	0.98	1036	337.0	40.3
2	ethyl butanoate (23, 24, 26, 50, 53, 55, 58, 60–62, 65, 69–72)	4, 10, 12, 20, 25, 30, 37, 60, 70, 80	13/4.8	0.97	345	0.99	937	318.6	49.2
3	ethyl 2-methylpropanoate (24)	4, 10, 20	3/161	1.00	345	1.00	643	307.3	52.8
4	ethyl hexanoate (23–26, 55, 58, 70, 71, 73–80)	0, 4, 10, 14, 20, 25, 30, 37	9/5.6	0.95	133	0.99	874	305.8	55.1
5	ethyl octanoate (71, 78, 80)	4, 20, 25	3/161	0.99	195	0.99	95.4	288.6	44.8
6	butan-2-one (69, 72, 81)	37, 60, 70, 80	4/18.5	0.99	367	1.00	452	364.3	38.9
7	hexan-2-one (69, 81)	37, 60, 70, 80	4/18.5	1.00	1115	1.00	518	339.0	41.9
8	octan-2-one (69, 72, 81)	37, 60, 70, 80	4/18.5	1.00	1542	1.00	1279	321.8	52.5
9	nonan-2-one (75, 82–84)	25, 30, 37	3/161	0.83	4.8	0.90	9.5 ^b	310.0	57.6
10	hexanal (24, 27, 50, 65, 71, 72, 82, 85)	4, 20, 30, 35, 37, 40, 60, 70, 80	10/5.3	0.92	91.0	0.97	279	330.7	48.0
11	octanal (68, 80–82, 85, 86)	20, 25, 30, 37, 40	5/10.1	0.98	180	0.99	299	304.6	67.7
12	butan-1-ol (50, 54, 60, 72, 82, 87–91)	20, 25, 35, 37, 40, 50, 60, 70, 80	9/6	0.85	40.3	0.97	201	377.7	58.0
13	(3Z)-hex-3-en-1-ol (cis-3-hexenol) (23, 26)	12, 20, 25, 30, 37	5/10.1	0.81	12.8	0.90	27.5	374.4	59.4
14	hexan-1-ol (69, 72, 81)	37, 60, 70, 80	4/18.5	0.99	242	0.99	272	357.9	65.2

^a T_{eq} , temperature of change of equilibrium shifting. ^b F test < F_{crit} , nonsignificant regression.

computed using the predicted values of the missing molecules (the cross-validated $\text{CV-}r^2$):

$$\text{CV-}r^2 = 1 - \frac{\sum_{i=1}^n (y_{\text{exptl}} - y_{\text{pred}})^2}{\sum_{i=1}^n (y_{\text{exptl}} - \bar{y})^2}$$

Instead of repeatedly analyzing subsets of the data, bootstrapping repeatedly analyzes subsamples of the data. Each subsample is a random sample with replacement from the full sample.

The statistical significance provided by Y randomization is given by the equation

$$\text{significance} = \left[\frac{1 - (1 + x)}{y} \right] \times 100$$

where x = total number of trials providing a r^2 value lower than the initial trial and y = total number of trials (initial trial + random trials).

To obtain 99% confidence level, 99 random trials are generated ($y = 99$), and every generated trial is submitted to QSAR generation model using the same experimental conditions (functions and parameters) as the initial trial.

Visualization was performed with Viewer Pro 6.0 (Accelrys Inc.).

RESULTS AND DISCUSSION

Results of Calculation. *Gas/Water Partition Coefficient.* Data were collected in the literature for the 14 compounds and expressed as molar concentration. A comprehensive conversion of gas/water partition coefficient was recently reported for ethyl butyrate (8) and was applied in the present study for the other aroma compounds.

For each aroma compound, a linear equation was obtained for the regression between $\ln K$ and $1/T$ and led to equilibrium thermodynamic standard values for the 14 aroma compounds in water (Table 2). For all investigated aroma compounds, correlation coefficients are between 0.81 and 1.00, and thus the equation of the linear regression can be used to predict gas/water partition coefficients at temperatures other than those of the experimental measurements. The $\ln K_{\text{calcd}}$ values are determined for each experimental temperature using $\ln K_{\text{exptl}}$ versus $1/T$ equations. We checked that experimental and calculated $\ln K$ values were strongly correlated (Table 2).

Figure 1 shows as example the regression plots obtained for esters. The slopes are almost the same, indicating few differences between ΔH° values. The curves differ only in their intercepts, which are related to $\ln K$ values.

Enthalpies Variation Values. The linear relationship between $\ln K_{\text{exptl}}$ and $1/T$ indicates that in the temperature range studied, the enthalpies of vaporization can be considered as constant according to Ellingham's approximation (23).

Vaporization enthalpy values of aroma compounds in water calculated according to van't Hoff's law and entropy vaporization are reported in Table 2.

For ethyl acetate, ethyl butanoate, and ethyl hexanoate, the calculated enthalpy values (respectively equal to 40.3, 49.2, and 55.1 kJ mol^{-1}) are in good agreement with those previously published [ethyl acetate, 52 kJ mol^{-1} (24), 39.3 kJ mol^{-1} (23), 52 kJ mol^{-1} (25); ethyl butanoate, 50.9 kJ mol^{-1} (24), 46.7 kJ mol^{-1} (26); ethyl hexanoate, 45.5 kJ mol^{-1} (26), 63 kJ mol^{-1} (25)].

The enthalpy value calculated for hexanal (equal to 48 kJ mol^{-1}) is included in the range defined by the previous determinations [40.4 kJ mol^{-1} (27); 64 kJ mol^{-1} (24)], and the $\Delta H_{\text{eq}}^\circ$ value calculated for (3Z)-hex-3-en-1-ol (58 kJ mol^{-1}) is also close to that reported by Phillippe et al. [64.7 kJ mol^{-1} (23)].

Comparison of Thermodynamic Values for Pure Aroma Compounds and Compounds in Aqueous Solution. We compared the thermodynamic values of vaporization for the 14 compounds in pure medium and in aqueous solution (Table 1 and Table 2).

The $\log K_{\text{liq},30^\circ\text{C}}$ and $\log K_{\text{ret},30^\circ\text{C}}$ values are displayed in Figure 2. This graphical representation reveals an apparent "symmetrical effect" due to the difference between volatility of pure aroma compounds and aroma compounds in aqueous solution that exists for the largest molecules (ethyl hexanoate, ethyl octanoate, octan-2-one, nonan-2-one, and octanal). Indeed, the balance between liquid and vapor phases is reversed according to the composition of the liquid phase (pure compounds or compounds in aqueous solution), so that it shifts widely to the pure liquid phase and widely to the vapor phase in aqueous medium. The behaviors of the smallest molecules (ethyl acetate, butan-2-one, butan-1-ol) differ: for ethyl acetate and butan-1-ol, the liquid–vapor balance is independent of the medium, whereas butan-2-one constitutes the only case of the 14 studied compounds

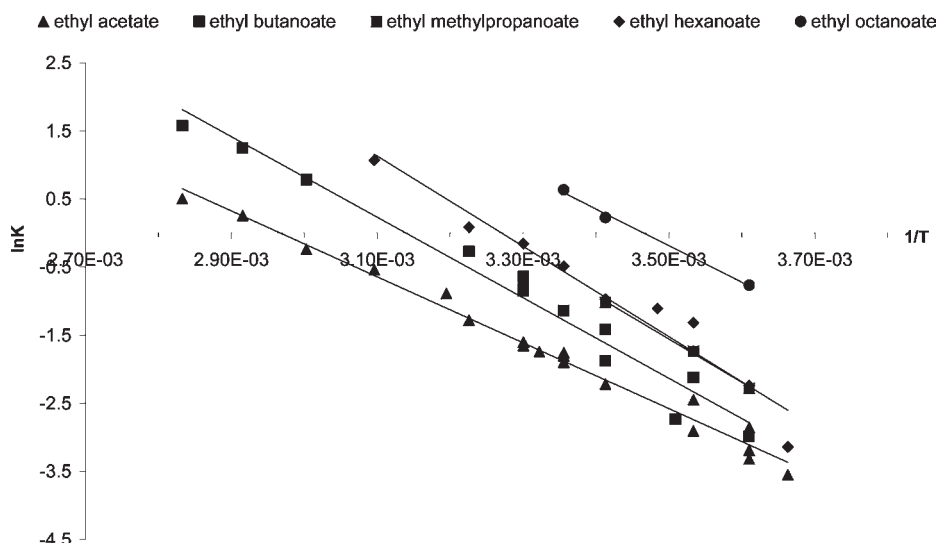


Figure 1. Relationship between $\ln K$ and $1/T$ for investigated esters.

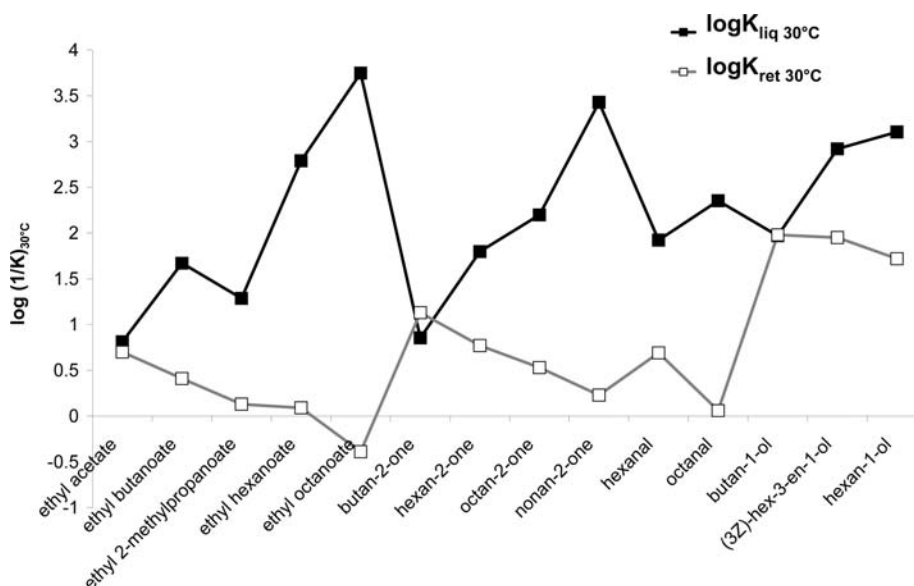


Figure 2. $\log K_{\text{liq},30^\circ\text{C}}$ and $\log K_{\text{ret},30^\circ\text{C}}$ values for investigated aroma compounds.

for which the liquid/vapor balance toward liquid phase is faintly improved in aqueous solution.

Figure 3 shows the energy values of equilibrium at 30°C for pure compounds (a) and compounds in aqueous solution (b). Enthalpy values are narrowly distributed in a range of 28.8 kJ mol^{-1} , varying from 38.9 to 67.7 kJ mol^{-1} , whereas entropy values are proportionately distributed in a larger range of $115.4\text{ J K}^{-1}\text{ mol}^{-1}$, from 106.9 to $222\text{ J K}^{-1}\text{ mol}^{-1}$. Mean values of enthalpy and entropy are respectively equal to 52 kJ mol^{-1} and $158\text{ J K}^{-1}\text{ mol}^{-1}$.

$\Delta H_{\text{eq}}^\circ$ values are higher than $\Delta H_{\text{vap}}^\circ$ values except for ethyl octanoate. Within each chemical class, we observed an increase in enthalpy value with the increase of the number of carbon atoms in the chain, except for the pure branched molecule ethyl 2-methylpropanoate, ethyl octanoate in aqueous solution, pure octan-2-one, and pure aldehydes.

Indeed, the vaporization enthalpy of pure ethyl 2-methylpropanoate is lower than that of its linear isomer ethyl butanoate and close to vaporization enthalpy value of ethyl acetate (enthalpy values equal, respectively, to 35.6 , 42 , and 35 kJ mol^{-1}). In aqueous solution, the vaporization enthalpy value is higher for ethyl 2-methylpropanoate ($\Delta H_{\text{eq}}^\circ = 52.8\text{ kJ mol}^{-1}$) than for

ethyl butanoate ($\Delta H_{\text{eq}}^\circ = 49.2\text{ kJ mol}^{-1}$). Conversely, the highest vaporization enthalpy value corresponds to ethyl octanoate ($\Delta H_{\text{vap}}^\circ = 59\text{ kJ mol}^{-1}$) for pure esters, but to ethyl hexanoate ($\Delta H_{\text{vap}}^\circ = 55.1\text{ kJ mol}^{-1}$) for esters in aqueous solution.

The vaporization enthalpy of pure octan-2-one ($\Delta H_{\text{vap}}^\circ = 39.8\text{ kJ mol}^{-1}$) is lower than vaporization enthalpy of hexan-2-one and nonan-2-one (respectively equal to 43 and 56.44 kJ mol^{-1}), whereas in aqueous solution the vaporization enthalpy value of octan-2-one ($\Delta H_{\text{eq}}^\circ = 52.5\text{ kJ mol}^{-1}$) is between enthalpy values of hexan-2-one ($\Delta H_{\text{eq}}^\circ = 41.9\text{ kJ mol}^{-1}$) and nonan-2-one ($\Delta H_{\text{eq}}^\circ = 57.6\text{ kJ mol}^{-1}$).

Hierarchical order of values is also reversed for aldehydes: the vaporization enthalpy of pure hexanal is slightly higher than the vaporization enthalpy of pure octanal (respectively equal to 45.3 and 43 kJ mol^{-1}); aqueous medium does not change the vaporization enthalpy of hexanal ($\Delta H_{\text{eq}}^\circ = 48\text{ kJ mol}^{-1}$) but dramatically increases the vaporization enthalpy of nonanal ($\Delta H_{\text{eq}}^\circ = 67.7\text{ kJ mol}^{-1}$).

The range of entropy values is also close for pure compounds (89.2 – $141.9\text{ J K}^{-1}\text{ mol}^{-1}$), but larger for compounds in aqueous solution (106.9 – $222.3\text{ J K}^{-1}\text{ mol}^{-1}$), and $\Delta S_{\text{eq}}^\circ$ values are higher

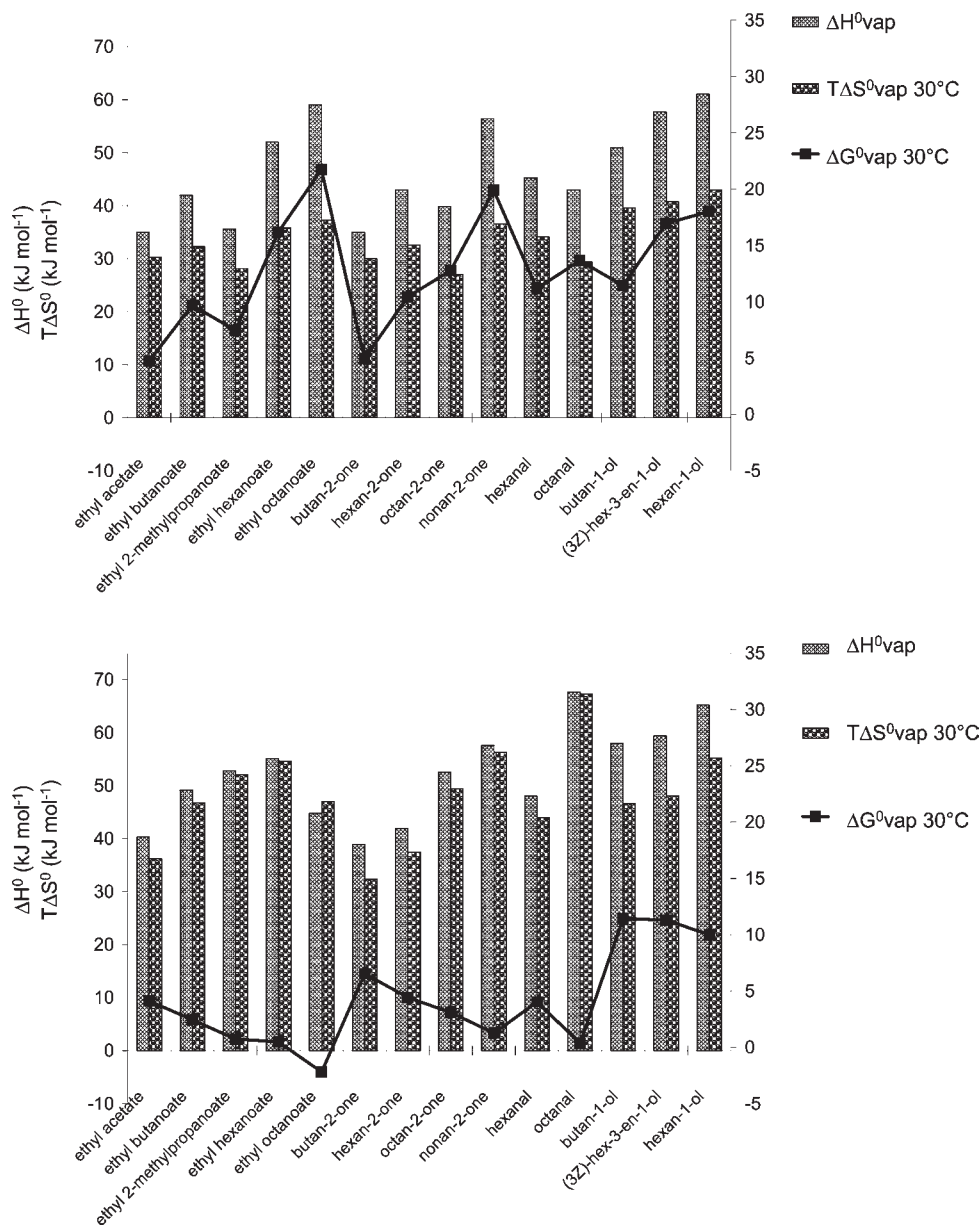


Figure 3. Thermodynamic standard equilibrium values ΔH° , $T\Delta S^\circ$, and ΔG° at 30 °C for pure compounds (a, top) and compounds in aqueous solutions (b, bottom).

than $\Delta S^\circ_{\text{vap}}$ values. According to the molecular structures, we observed the same variations for entropy values as for enthalpy values, as well for pure compounds and compounds in aqueous solution.

At 30 °C, the entropic term $T\Delta S^\circ$ is lower than the enthalpic term ΔH° for each pure compound, so that the vaporization free enthalpy value is positive for all pure compounds and increases with the increase of the length of carbon chain in the same chemical family. Conversely, for compounds in aqueous solution the entropic term value is lower but close to the enthalpic term value, except for ethyl octanoate, for which the entropic term is higher than the enthalpic term. In this way, the vaporization free enthalpy value decreases with the increase of the length of carbon chain and becomes negative for ethyl octanoate.

Interestingly, we observed some compounds for which $\Delta G^\circ_{30^\circ\text{C}}$ values are very close, whereas ΔH° and ΔS° values are different. It is the case for pure hexanal and butan-1-ol (Figure 3a), on the one hand ($\Delta G^\circ_{\text{liq},30^\circ\text{C}}$ values equal to 11.16 and 11.44 kJ mol⁻¹, respectively), and, on the other hand, for hexanal and ethyl

acetate in aqueous solution (Figure 3b) ($\Delta G^\circ_{\text{eq},30^\circ\text{C}}$ values equal to 4.11 and 4.04 kJ mol⁻¹, respectively).

For a better investigation of enthalpy and entropy values, we focused on the differences between $\Delta H^\circ_{\text{vap}}$ and $\Delta H^\circ_{\text{eq}}$, on the one hand, and $\Delta S^\circ_{\text{vap}}$ and $\Delta S^\circ_{\text{eq}}$, on the other hand. Histograms of $(\Delta H^\circ_{\text{eq}} - \Delta H^\circ_{\text{vap}})$ and $(\Delta S^\circ_{\text{eq}} - \Delta S^\circ_{\text{vap}})$ values, denoted, respectively, $\Delta\Delta H^\circ$ and $\Delta\Delta S^\circ$, are displayed in Figure 4.

$\Delta\Delta H^\circ$ values are negative for ethyl octanoate (−14.20 kJ mol⁻¹) and hexan-2-one (−1.10 kJ mol⁻¹). The highest absolute values are assumed by several large molecules (ethyl octanoate, octan-2-one, octanal; absolute $\Delta\Delta H^\circ$ values equal, respectively, to 14.2, 12.7, and 24.7 kJ mol⁻¹) but also by ethyl 2-methylpropanoate (MW = 116 g mol⁻¹, $\Delta\Delta H^\circ = 17$ kJ mol⁻¹). Nonetheless, the $\Delta\Delta H^\circ$ value is middle for ethyl butanoate (MW = 116 g mol⁻¹, $\Delta\Delta H^\circ = 7.20$ kJ mol⁻¹) and low for nonan-2-one (MW = 142 g mol⁻¹, $\Delta\Delta H^\circ = 1.16$ kJ mol⁻¹). There is no relationship between the size of the molecule and the difference between enthalpy values.

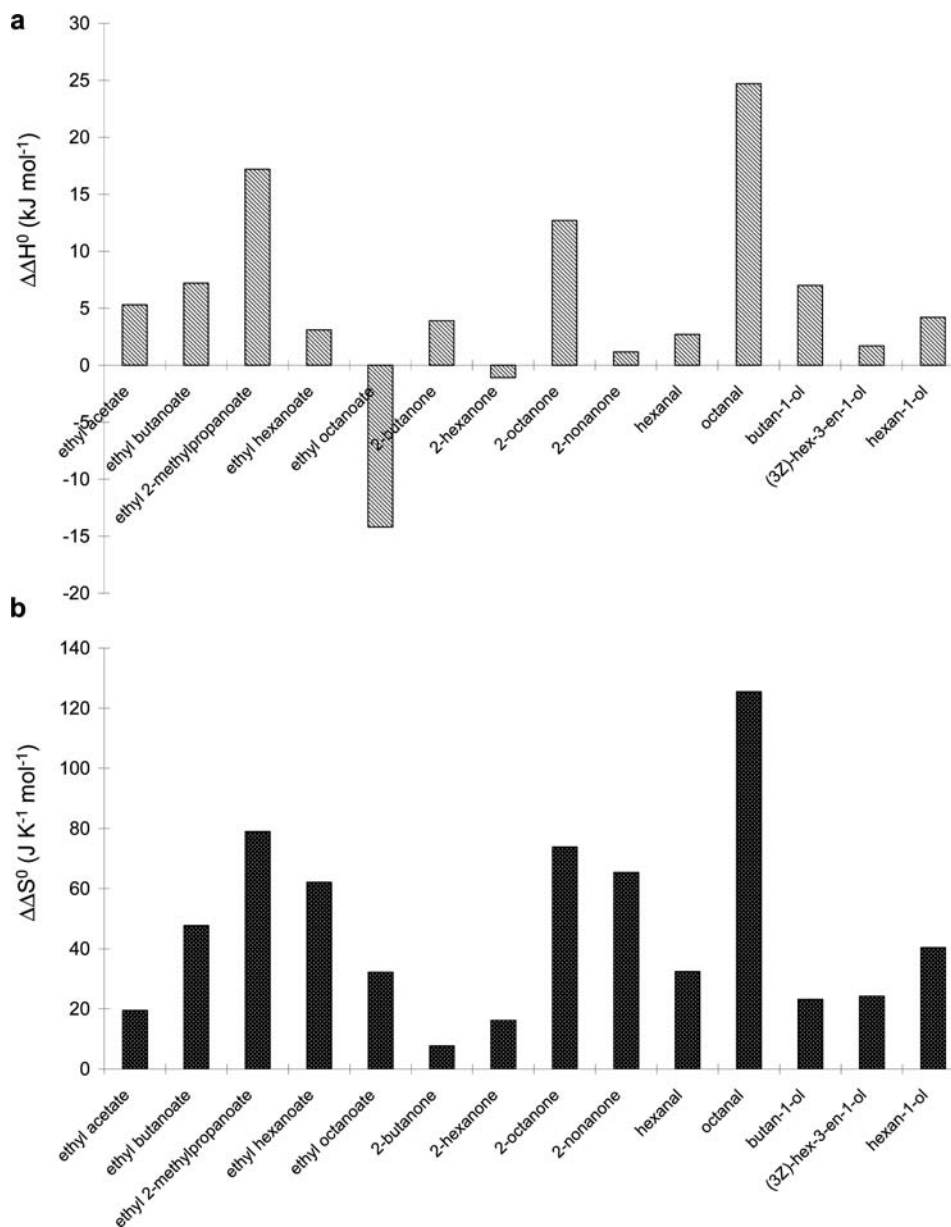


Figure 4. Differences between enthalpy values $\Delta\Delta H^\circ$ (a) and entropy values $\Delta\Delta S^\circ$ (b).

On the other hand, the smallest $\Delta\Delta S^\circ$ value corresponds to the smallest molecule (butan-2-one, $\text{MW} = 72 \text{ g mol}^{-1}$, $\Delta\Delta S^\circ = 7.70 \text{ J K}^{-1} \text{mol}^{-1}$) and the highest value to a large molecule (octanal, $\text{MW} = 128 \text{ g mol}^{-1}$, $\Delta\Delta S^\circ = 125.45 \text{ J K}^{-1} \text{mol}^{-1}$), but not to the largest molecule (ethyl octanoate, $\text{MW} = 172 \text{ g mol}^{-1}$, $\Delta\Delta S^\circ = 32.18 \text{ J K}^{-1} \text{mol}^{-1}$). Conversely to what was observed for the $\Delta\Delta H^\circ$ values, there is a link between the differences between $\Delta S^\circ_{\text{vap}}$ and $\Delta S^\circ_{\text{cq}}$ and molecule size, except for ethyl octanoate.

To better understand enthalpy and entropy vaporization meaning, it is necessary to introduce the hydrophobic effect, so that the characteristic of interaction between water and hydrophobic molecules is considered.

To describe the solvation of a hydrophobic molecule in water, Frank and Evans (28) have proposed the “iceberg” model. Several modifications of the iceberg model have been suggested (29–35). Despite their differences, these models are in good agreement on several points: (1) Water molecules form a cage around hydrophobic molecules; some authors use the paradoxical term “hydrophobic hydration”. (2) At room temperature,

the water structure is more ordered in the presence of a hydrophobic molecule than pure water (the term “iceberg” refers, in fact, to a “crystallinity” of aqueous solution). (3) The aqueous solution has a larger heat capacity than pure water.

Our observations are in good agreement with these elements. Indeed, the positive $\Delta\Delta H^\circ$ values observed for all compounds of our training set, except ethyl octanoate and hexan-2-one, could be interpreted as the supplementary energy required to break the cages of water around the solute molecules before its evaporation. In the “iceberg” model of aqueous solution, the positive $\Delta\Delta S^\circ$ values reflect the higher organization level in aqueous solution and restricted degree of freedom of hydrophobic molecules in the water clathrate.

We examined the correlations between the thermodynamical values [$\log(1/K)$, T , ΔH° , ΔS°] obtained for the compounds of the training set: the correlation matrix between values is reported in **Table 3**.

We observed for each medium a strong correlation, on the one hand, between T and $\log(1/K)$ values and, on the other hand, between ΔH° and ΔS° both for pure compounds and for

compounds in aqueous solution (r values > 0.89). This enthalpy–entropy correlation could be related to the enthalpy–entropy compensation phenomenon that is a well-known rule of behavior probably due to weak intermolecular interactions (36).

For pure compounds, $\Delta H^\circ_{\text{vap}}$ appeared to be highly correlated with $\log K_{\text{liq}}$ ($r = 0.91$) and also correlated with T_{vap} ($r = 0.71$), whereas no good correlation exists either between $\Delta S^\circ_{\text{vap}}$ and $\log K_{\text{liq}}$ or between $\Delta S^\circ_{\text{vap}}$ and T_{vap} . Moreover, $\Delta S^\circ_{\text{vap}}$ values are almost the same for the compounds of the training set (Figure 3a). Taken together, these results highlight a key role of enthalpy in vaporization phenomenon of pure compounds.

The situation seems to be different for compounds in aqueous solution. Indeed, no correlation exists, respectively, between $\ln K_{\text{liq},30^\circ\text{C}}$ and $\ln K_{\text{ret},30^\circ\text{C}}$ ($r = -0.13$), between T_{eq} and $\Delta H^\circ_{\text{eq}}$ ($r = 0.02$), and between $\log K_{\text{ret},30^\circ\text{C}}$ and $\Delta H^\circ_{\text{eq}}$ ($r = 0.21$); moreover, at 30 °C, the entropy term is very close to the enthalpy term (Figure 3b) with $\Delta S^\circ_{\text{eq}}$ values belonging to a large range (68–222 J K⁻¹ mol⁻¹). This observation puts forward the role of entropy in the balance shift between vapor and liquid phase for vaporization of compounds in aqueous solution.

The absence of good correlation between $\Delta H^\circ_{\text{vap}}$ and $\Delta H^\circ_{\text{eq}}$ ($r = 0.51$), on the one hand, and between $\Delta S^\circ_{\text{vap}}$ and $\Delta S^\circ_{\text{eq}}$ ($r = 0.15$), on the other hand, is more difficult to interpret. The entropy values depend on the degree of freedom of the molecules. In this way, the entropy variation corresponding to the displacement of a molecule from liquid phase to vapor phase reflects the change in conformational freedom of the molecule between the two phases. The conformational freedom in vapor phase is obviously the same whether the molecule comes from pure or

aqueous medium. Conversely, there is a great difference of conformational space between pure liquid compound and the same molecule in aqueous solution. Because of the difference in the nature of the interactions, no simple relationship exists between the conformational freedoms in the two media.

Chemistry: Structure–Property Study. We used a structure–activity relationship approach using QSAR tools provided by the Cerius² package (Accelrys) to evaluate the influence of the chemical structure of aroma compounds on the thermodynamic values of retention/release equilibrium between vapor phase and liquid phase ($\log K_{\text{liq},30^\circ\text{C}}$, T_{vap} , $\Delta H^\circ_{\text{vap}}$, and $\Delta S^\circ_{\text{vap}}$; and $\log K_{\text{ret},30^\circ\text{C}}$, T_{eq} , $\Delta H^\circ_{\text{eq}}$, and $\Delta S^\circ_{\text{eq}}$ values, for pure compounds and compounds in aqueous solutions, respectively).

We performed simple linear regressions on the whole set of 14 compounds, on the 5-ester subset (compounds 1–5) and on the 4-ester subset after removal of ethyl octanoate (compounds 1–4) (37–39). Indeed, this compound has the peculiarity to present a $\Delta H^\circ_{\text{ret}}$ value lower than $\Delta H^\circ_{\text{vap}}$ value (Tables 1 and 2).

We retained nine descriptors that present the best simple linear correlations with at least one thermodynamic property for at least one training set. The obtained best equations, displayed in Table 4, have been validated at 99% confidence level by Y scrambling. To these nine descriptors, we added AlogP98, RadOfGyration, Jurs-SASA, and Jurs-TPSA. Indeed, the global hydrophobicity (AlogP98) is a classical largely used descriptor in structure–property relationship studies. The shape descriptors RadOfGyration, solvent accessible surface area (Jurs-SASA), and total polar surface area (Jurs-TPSA) are interesting molecular properties because they are conformation-dependent descriptors and could so provide information about the relationship between conformation and property (12, 40–42). The definitions and meanings of the 13 descriptors are reported in Table 5, descriptor values are reported in Table 6, and the correlation matrix is reported in Table 7. Although several descriptors are strongly correlated (for example, RadOfGyration, Jurs-SASA, and CHI-V-1; and PHI and RotBond), we have retained all 13 because the use of simple linear regression avoids the risk of collinearity and overfitting as occurs in multilinear regression (43).

Temperature of Balance Shift and Constant Equilibrium Values. T_{vap} and $\log K_{\text{liq},30^\circ\text{C}}$ are highly correlated ($r = 0.93$), and the best correlations were respectively obtained with Rotlbonds

Table 3. Correlation Matrix between Thermodynamic Values

	T_{vap}	$\log K_{\text{liq},30^\circ\text{C}}$	$\Delta H^\circ_{\text{vap}}$	$\Delta S^\circ_{\text{vap}}$	T_{eq}	$\log K_{\text{ret},30^\circ\text{C}}$	$\Delta H^\circ_{\text{eq}}$	$\Delta S^\circ_{\text{eq}}$
T_{vap}	1							
$\log K_{\text{liq},30^\circ\text{C}}$	0.93	1						
$\Delta H^\circ_{\text{vap}}$	0.71	0.91	1					
$\Delta S^\circ_{\text{vap}}$	0.34	0.64	0.90	1				
T_{eq}	-0.50	-0.28	0.06	0.41	1			
$\log K_{\text{ret},30^\circ\text{C}}$	-0.36	-0.13	0.21	0.53	0.97	1		
$\Delta H^\circ_{\text{eq}}$	0.51	0.53	0.51	0.40	0.02	0.21	1	
$\Delta S^\circ_{\text{eq}}$	0.67	0.58	0.41	0.15	-0.43	-0.27	0.89	1

Table 4. QSAR Equations of Thermodynamic Standard Values versus Descriptors

thermodynamic values	equations	r^2	F test ^a	CV- r^2	BS- r^2
whole set (14 compounds)					
T_{vap} (K)	$328.402 + 20.2096 * \text{“Rotlbonds”}$	0.90	108	0.86	0.90
$\log K_{\text{liq}}$	$-0.012594 + 0.434849 * \text{“PHI”}$	0.79	45	0.72	0.79
$\Delta H^\circ_{\text{vap}}$ (J mol ⁻¹)	$-29916.5 + 587254 * \text{“Jurs-FPSA-3”}$	0.56	15	0.39	0.56
$\Delta S^\circ_{\text{vap}}$ (J K ⁻¹ mol ⁻¹)	$-22.9784 + 1035.67 * \text{“Jurs-FPSA-3”}$	0.56	15	0.41	0.56
T_{eq} (K)	$245.991 + 340.448 * \text{“Jurs-RNCG”}$	0.82	56	0.77	0.82
$\log K_{\text{ret}}$	$-1.39658 + 8.42893 * \text{“Jurs-RNCG”}$	0.74	34	0.65	0.74
$\Delta H^\circ_{\text{eq}}$ (J mol ⁻¹)	$-17513.2 + 533675 * \text{“Jurs-FPSA-3”}$	0.49	12	0.35	0.49
$\Delta S^\circ_{\text{eq}}$ (J K ⁻¹ mol ⁻¹)	$99.3242 + 11.6594 * \text{“PHI”}$	0.52	13	0.20	0.52
$T_{\text{vap}} - T_{\text{eq}}$ (K)	$-111.473 + 62.653 * \text{“CHI-V-1”}$	0.99	1184	0.98	0.99
$\log K_{\text{liq}}/K_{\text{ret}}$	$-2.57756 + 1.30512 * \text{“CHI-V-1”}$	0.97	364	0.96	0.97
5-esters subset					
$\Delta H^\circ_{\text{vap}}$ (J mol ⁻¹)	$21975.9 + 4437.97 * \text{“PHI”}$	0.99	224	0.96	0.99
$\Delta H^\circ_{\text{eq}}$ (J mol ⁻¹)	$210277 + 5593.14 * \text{“Jurs-PNSA-3”}$	0.78	10.7	0.56	0.76
$\Delta\Delta H^{cb}$ (J mol ⁻¹)	$34170.8 - 5394.55 * \text{“Kappa-3-AM”}$	0.93	43	0.79	0.92
4-esters subset					
$\Delta H^\circ_{\text{eq}}^c$ (J mol ⁻¹)	$30629.1 + 11263.3 * \text{“CHI-V-2”}$	0.98	78	0.80	0.99
$\Delta H^\circ_{\text{eq}}^d$ (J mol ⁻¹)	$77683.2 - 138337 * \text{“Jurs-RPSA”}$	0.97	65	0.94	0.93

^a F_{crit} values: for 14 observations $F_{\text{crit}} = 4.7$; for 5 observations $F_{\text{crit}} = 10$; for 4 observations $F_{\text{crit}} = 18.5$. ^b Nonsignificant correlation with Kappa-3-AM for the whole set ($r^2 = 0.14$). ^c Nonsignificant correlation with CHI-V-2 for the 5-esters subset ($r^2 = 0.12$). ^d Nonsignificant correlation with Jurs-RPSA for the 5-esters subset ($r^2 = 0.32$).

Table 5. Meaning of Descriptors

descript	family	information
RadOfGyration	spatial	radius of gyration of the molecule
Jurs-SASA	spatial	total molecular solvent-accessible area
Jurs-PNSA-3	spatial	atomic charge weighted negative surface area: sum of the product of solvent-accessible surface area \times partial charge for all negatively charged atoms, $\sum_s Q_s^- \times SA_s^-$
Jurs-FPSA-3	spatial	fractional positive charged partial surface areas: atomic charge weighted positive surface area: sum of the product of solvent-accessible surface area \times partial charge for all positively charged atoms, and divided by the total molecular solvent-accessible surface area (SASA), $Jurs-PPSA-3/Jurs-SASA = \sum_r Q_r^+ \times SA_r^+ / Jurs-SASA$
Jurs-RNCG	spatial	relative negative charge: charge of most negative atom divided by the total negative charge, $Jurs-RNCG = \text{charge of most negative atom} / \text{total negative charge} = Q_{\max}^- / Q^-$
Jurs-TPSA	spatial	total polar surface area: sum of solvent-accessible surface areas of atoms with absolute value of partial charges ≥ 0.2 , $Jurs-TPSA = \sum_a SA_a; \forall a: q_a \geq 0.2$
Jurs-RPSA	spatial	relative polar surface area: total polar surface area divided by the total molecular solvent-accessible surface area, $Jurs-RPSA = Jurs-TPSA / Jurs-SASA$ Jurs TPSA, total polar surface area, sum of solvent-accessible surface areas of atoms with absolute value of partial charges ≥ 0.2 , $Jurs-TPSA = \sum_a SA_a; \forall a: q_a \geq 0.2$
Rotlbonds	structural	number of rotatable bonds
AlogP98	thermodynamic	log of the octanol/water partition coefficient is related to the hydrophobic character of the molecule (calculated using an atom-type value based approach)
PHI	topological	flexibility index
Kappa-3-AM	topological	Kier's shape indice order 3 α -modified Kappa-3-AM indices are refinements of Kappa-3 index that take into account the contribution of the covalent radii and hybridization states
CHI-V-1	topological	first-order Kier and Hall molecular connectivity index valence-modified ^a CHI-V-1 indices encode the number of bonds (assume nonzero values for compounds having bonds to be connected to the skeletal atoms)
CHI-V-2	topological	second-order Kier and Hall molecular connectivity index valence-modified ^a CHI-V-2 indices encode the number of pairs of bonds (assume nonzero values for compounds having two bonds to be connected)

^a Kier and Hall connectivity index was originally defined by Randić (92). Connectivity indices take into account the number of its electrons in sigma bonds and the valence-modified connectivity index. CHI-V is a refinement of the molecular connectivity index that takes into account the presence of heteroatoms.

Table 6. Descriptors Values

no.	compound	RadOf Gyration	Jurs-SASA	Jurs-PNSA-3	Jurs-FPSA-3	Jurs-RNCG	Jurs-TPSA	Jurs-RPSA	Rotl bonds	AlogP98	PHI	Kappa -3-AM	CHI-V-1	CHI-V-2
1	ethyl acetate	2.410	275.0	-30.45	0.1142	0.3305	74.38	0.2704	2	0.370	2.670	5.010	1.90	0.925
2	ethyl butanoate	3.111	338.6	-28.86	0.1344	0.2370	66.59	0.1966	4	1.493	4.560	4.630	2.96	1.555
3	ethyl 2-methylpropanoate	2.739	331.2	-27.90	0.1253	0.2400	63.05	0.1903	3	1.499	3.440	3.339	2.85	1.907
4	ethyl hexanoate	3.782	396.6	-28.49	0.1346	0.1892	64.17	0.1618	6	2.405	6.50	6.630	3.97	2.262
5	ethyl octanoate	4.461	458.8	-28.97	0.1371	0.1578	65.30	0.1423	8	3.318	8.46	8.630	4.97	2.969
6	butan-2-one	2.052	246.5	-23.28	0.1090	0.3355	58.89	0.2390	1	0.563	1.81	3.670	1.77	1.056
7	hexan-2-one	2.709	309.2	-25.32	0.1208	0.2360	62.00	0.2005	3	1.475	3.67	5.670	2.77	1.806
8	octan-2-one	3.393	397.5	-25.87	0.1252	0.1834	63.51	0.1705	5	2.388	5.59	7.670	3.77	2.513
9	nonan-2-one	3.741	372.4	-24.67	0.1276	0.1651	59.21	0.1490	6	2.844	6.56	8.820	4.27	2.866
10	hexanal	2.648	310.7	-28.20	0.1296	0.2264	60.21	0.1938	4	1.853	5.40	5.670	2.86	1.662
11	octanal	3.338	373.7	-28.65	0.1329	0.1774	60.93	0.1631	6	2.765	7.39	7.670	3.86	2.370
12	butan-1-ol	2.205	309.5	-24.83	0.1522	0.3894	68.37	0.2632	3	0.971	3.93	3.960	2.02	1.077
13	(3Z)-hex-3-en-1-ol	2.779	326.9	-27.59	0.1406	0.3373	76.31	0.2465	4	1.439	5.46	5.700	2.67	1.392
14	hexan-1-ol	2.833	259.8	-22.29	0.1464	0.3011	78.97	0.2416	5	1.883	5.93	5.960	3.02	1.784

($r^2 = 0.90$, F test = 108) and PHI ($r^2 = 0.79$, F test = 45). These two descriptors are strongly correlated ($r = 0.98$) and have a similar meaning. Indeed, Rotlbonds encodes the number of rotatable bonds in the molecule, whereas PHI encodes the molecular flexibility as restriction from being "infinitely flexible molecule" and strongly depends of number of rotatable bonds. Positive correlations of these two indices with T_{vap} and $\log K_{\text{liq},30^\circ\text{C}}$ indicate that the higher the degree of flexibility, the higher the shifting of the equilibrium to liquid phase. In this way, the flexibility allows intermolecular contact optimization and improves the stability of the liquid phase for the present set of compounds.

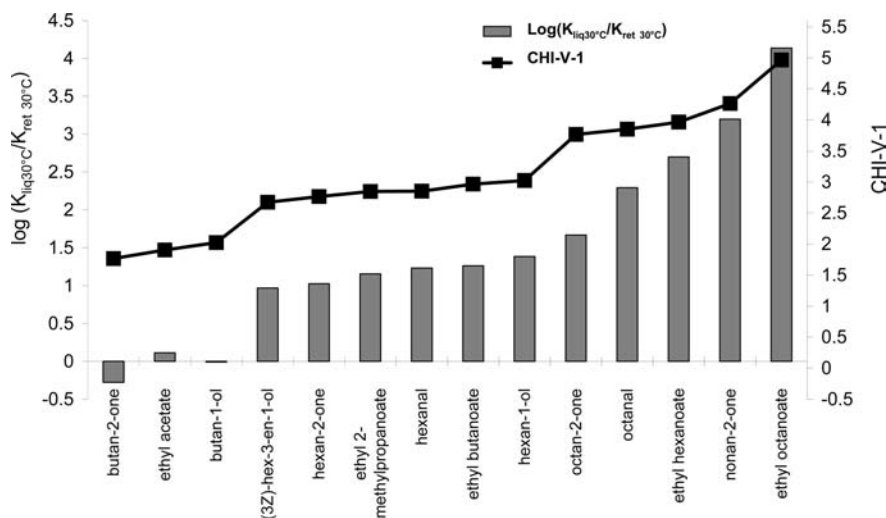
AlogP98 is also correlated with T_{vap} (predicted $T_{\text{vap}} = 336.8876 + 43.2906 \text{ AlogP98}$; $r^2 = 0.90$, F test = 103) but poorly

with $\log K_{\text{liq},30^\circ\text{C}}$ (predicted $\log K_{\text{liq},30^\circ\text{C}} = 0.656546 + 0.857296 \text{ AlogP98}$; $r^2 = 0.67$, F test = 23.8). High values of AlogP98 are characteristic of molecules able to involve van der Waals hydrophobic interactions, and van der Waals forces ensure the cohesion between hydrophobic molecules and, so, improve the stability of the pure liquid state. In this way, the correlation between AlogP98 and T_{vap} has the same meaning as correlation between Rotlbond and T_{vap} . Conversely, the molecular flexibility best explains the stability in pure liquid phase than the global hydrophobicity.

For compounds in aqueous solution, both T_{eq} and $\log K_{\text{ret},30^\circ\text{C}}$ are positively correlated with Jurs-RNCG, which means the higher the negative charge density, the higher the vaporization temperature and equilibrium displacement shift to liquid phase, leading to more retention in water (14). Indeed, Jurs-RNCG is a

Table 7. Correlation Matrix between Molecular Descriptors

	RadOfGyration	Jurs-SASA	Jurs-PNSA-3	Jurs-FPSA-3	Jurs-RNCG	Jurs-TPSA	Jurs-RPSA	Rotlbonds	AlogP98	PHI	Kappa-3-AM	CHI-V-1	CHI-V-2
RadOfGyration	1												
Jurs-SASA	0.99	1											
Jurs-PNSA-3	-0.30	-0.29	1										
Jurs-FPSA-3	0.22	0.22	0.10	1									
Jurs-RNCG	-0.84	-0.88	0.29	0.11	1								
Jurs-TPSA	-0.19	-0.22	0.00	0.46	0.55	1							
Jurs-RPSA	-0.85	-0.88	0.22	0.03	0.97	0.63	1						
Rotlbonds	0.94	0.94	-0.20	0.47	-0.75	-0.06	-0.76	1					
AlogP98	0.92	0.94	-0.11	0.32	-0.86	-0.30	-0.88	0.96	1				
PHI	0.87	0.87	-0.20	0.52	-0.69	-0.03	-0.70	0.98	0.94	1			
Kappa-3-AM	0.84	0.83	-0.09	0.14	-0.74	-0.17	-0.71	0.86	0.87	0.85	1		
CHI-V-1	0.98	0.99	-0.20	0.24	-0.88	-0.27	-0.90	0.96	0.98	0.90	0.87	1	
CHI-V-2	0.91	0.94	-0.07	0.13	-0.91	-0.39	-0.92	0.88	0.96	0.82	0.85	0.97	1

**Figure 5.** Release–retention constant equilibrium ratio $\log(K_{\text{liq},30^\circ\text{C}}/K_{\text{ret},30^\circ\text{C}})$ of the 14 aroma compounds sorted by increasing CHI-V-1 values.

spatial descriptor that encodes the electronic properties and charge distribution on the molecule (42). The smallest alcohol of the training set, butan-1-ol, assumes the highest Jurs-RNCG value (Jurs-RNCG = 0.3894), whereas the large ester ethyl octanoate takes the smallest value (Jurs-RNCG = 0.1578) (Table 6). Higher values of Jurs-RNCG correspond to the most polar molecules, and such a result points out the crucial role of polar interactions, which is coherent with the polar nature of water.

Figure 2 suggests that molecule shape has also an obvious function, insofar that the equilibrium shift to pure liquid is clearly lower for the branched isomer ethyl 2-methylpropanoate than for its linear isomer ethyl butanoate, whereas the difference between the retention of these two isomers is lower in aqueous solution. The role of molecular structure is demonstrated by the correlation observed between CHI-V-1 and both ($T_{\text{eq}} - T_{\text{vap}}$, $r^2 = 0.99$, F test = 1184) and $\log(K_{\text{liq},30^\circ\text{C}}/K_{\text{ret},30^\circ\text{C}})$, $r^2 = 0.97$, F test = 364). Chi connectivity indices, first proposed by Randić (44) and then developed by Kier and Hall (40, 44), represent molecular structure by encoding significant topological features of whole molecules. Indeed, CHI-V-1 encodes the number of bonds in the molecule and, in this way, the degree of branching, by expressing the possibility of each bond to connect to another bond of the molecule (45). Figure 5 displays the $\log(K_{\text{liq},30^\circ\text{C}}/K_{\text{ret},30^\circ\text{C}})$ values sorted by increasing CHI-V-1 values. The balance between liquid and vapor phases shifts widely to the pure liquid phase for molecules having CHI-V-1 values > 3.5, that is, octan-2-one,

octanal, ethyl hexanoate, nonan-2-one, ethyl octanoate (ranked by increase in CHI-V-1 values, Table 6). Displacement to aqueous phase occurs only for the smallest ketone (butan-2-one), which has the lowest CHI-V-1 value. In this way, the CHI-V-1 values explain how the structure of molecular carbon skeletons is related to the various differences between volatility of the molecules of pure aroma compounds and aroma compounds in aqueous solution, which appears as a “symmetrical effect” depicted in Figure 2. Thus, CHI-V-1 allows accurate descriptions of the behaviors of linear ester ethyl butanoate and its branched isomers ethyl 2-methylpropanoate.

Furthermore, we observed that the correlation between AlogP98 was satisfactory, although not as good [predicted $\log(K_{\text{liq},30^\circ\text{C}}/K_{\text{ret},30^\circ\text{C}}) = -0.97697 + 1.36665 \text{ AlogP98}$; $r^2 = 0.91$, F test = 116]. This result confirms that the structure chain explains more accurately than global hydrophobicity the balance between liquid and vapor phases.

Enthalpy and Entropy Values. We obtained only poor correlation between ΔH° or ΔS° and any molecular descriptor, for pure compounds as well as for compounds in aqueous solution (Table 4). Indeed, for pure compounds, the best correlation is obtained with Jurs-FPSA-3 ($r^2 = 0.56$, F test = 15) for both $\Delta H^\circ_{\text{vap}}$ and $\Delta S^\circ_{\text{vap}}$, whereas for compounds in aqueous solution $\Delta H^\circ_{\text{eq}}$ is also correlated with Jurs-FPSA-3 ($r^2 = 0.49$, F test = 11), and the best correlation for $\Delta S^\circ_{\text{eq}}$ is obtained with PHI ($r^2 = 0.52$, F test = 13). Especially for compounds in aqueous solution, these correlations are characterized by low

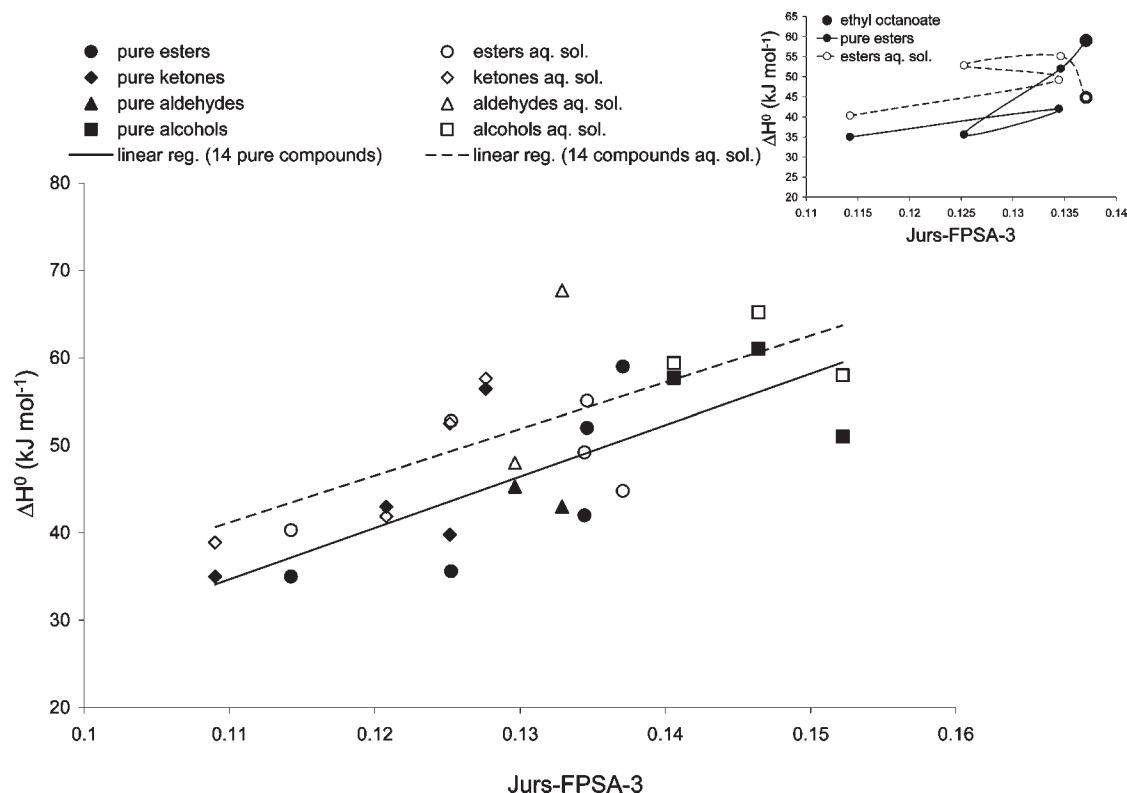


Figure 6. Regression plots of $\Delta H^{\circ}_{\text{eq}}$ and $\Delta H^{\circ}_{\text{vap}}$ versus Jurs-FPSA-3. The inset displays a zoom on the scatterplot of ΔH° values versus Jurs-FPSA-3 values. Connecting the dots improves visualization of ΔH° values variation according to the molecular structure.

statistical parameter values. No reliable correlations are obtained either for $\Delta\Delta H^{\circ}$ or for $\Delta\Delta S^{\circ}$ (predicted $\Delta\Delta H^{\circ} = -3365.76 + 2592.55$ Dipole-mag; $r^2 = 0.14$, F test = 1.9; predicted $\Delta\Delta S^{\circ} = 112.275 - 263.205$ Jurs-RNCG; $r^2 = 0.38$, F test = 7.5).

The meaning of the entropy variation role appears to be rather easy to understand. The entropy variation associated with a phase change reveals the difference in degree of conformational freedom between the two phases. For pure compounds, the small range of entropy values indicates few changes in conformational spaces between liquid and vapor phases for all of the compounds of the set. For compounds in aqueous solution, entropy values greatly vary according to their molecular structures. That means that in water the molecules have a lower conformational freedom than in pure liquid phase and recover their full conformational freedom when they reach the vapor phase. The range of variation of $\Delta S^{\circ}_{\text{vap}}$ values is rather small and seems to play a minor role compared to $\Delta H^{\circ}_{\text{vap}}$ in the equilibrium shift.

Despite its low reliability, the correlation between $\Delta S^{\circ}_{\text{eq}}$ and PHI underscores the major role played by the carbon chain length in the increase of degree of freedom in the vaporization behavior of the compounds in aqueous solution.

How To Interpret the Correlation between ΔH° and Jurs-FPSA-3? We focused on the correlations obtained for $\Delta H^{\circ}_{\text{vap}}$ and $\Delta H^{\circ}_{\text{eq}}$ values. The regression plots of ΔH° values versus Jurs-FPSA-3 (Figure 6) show that the two regression lines have almost parallel slopes, but the intercept of $\Delta H^{\circ}_{\text{eq}}$ versus Jurs-FPSA-3 has the highest value.

Jurs-FPSA-3 is a surface and electronic descriptor that encodes positively charged surface areas of the molecule and their charges, divided by the total accessible surface area.

$\Delta H^{\circ}_{\text{vap}}$ and $\Delta H^{\circ}_{\text{eq}}$ are both positively correlated with Jurs-FPSA-3, which means the higher the fractional positive charges, the more energy required to break intermolecular bonding. Indeed, the enthalpy variation is in fact the amount of energy

(heat) required to break out the intermolecular bonding. The enthalpy term results from an association of a cohesive energy and latent heat of vaporization (46). Aroma compounds are pure organic liquids, and for such compounds cohesion in the liquid state is due to van der Waals interactions.

With regard to the training set, it appeared that the highest values of Jurs-FPSA-3 correspond to alcohols, especially the smallest alcohol, butan-1-ol, and the lowest value to the smallest ketone, butan-2-one (Table 6). Note that these two molecules have hydrophobicity values lower than 1, which indicates weak hydrophobicity (AlogP98 values respectively equal to 0.56 and 0.97). Nevertheless, the correlation between $\Delta H^{\circ}_{\text{vap}}$ and Jurs-FPSA-3 should be consistent with the relationship between the molecular structure and the amount of energy necessary to break van der Waals interactions. Indeed, alcohols are polar molecules, and the alcoholic function allows them to involve hydrogen bonds that have higher energies than the van der Waals interactions. However, alcohols of the training set do not exhibit the highest $\Delta H^{\circ}_{\text{eq}}$, $\Delta H^{\circ}_{\text{vap}}$, and $\Delta\Delta H^{\circ}$ values in comparison to those of the other molecules studied in the present work (Figures 3 and 4).

It is more difficult to interpret the role of Jurs-FPSA-3 to describe the break of interactions for compounds in water solution, and the meaning of enthalpy variation values for compounds in aqueous solution appeared to be intricate. Moreover, the correlation is lower with $\Delta H^{\circ}_{\text{eq}}$ than with $\Delta H^{\circ}_{\text{vap}}$ (r^2 values respectively equal to 0.49 and 0.56). Indeed, it has been argued that negatively charged areas significantly participate in the interaction between hydrogen atoms of water (47, 48).

The $\Delta H^{\circ}_{\text{eq}}$ values are higher than the $\Delta H^{\circ}_{\text{vap}}$ values (except for ethyl octanoate and hexan-2-one), which appeared to be counter-intuitive. Indeed, despite T_{eq} values being lower than T_{vap} values (except for butan-2-one), vaporization of aroma compounds in aqueous solution requires a higher vaporization energy than vaporization of pure aroma compounds.

From **Figure 6**, it appeared to be impossible to easily differentiate the scatterplot related to $\Delta H_{\text{vap}}^{\circ}$ from that related to $\Delta H_{\text{eq}}^{\circ}$. Assuming that chemical function could be crucial, and because of the small size of the training set (it was not significant to examine the small subsets of ketones, aldehydes, and alcohols), we focused on the esters subset (37).

Esters Subset. The set of five esters allows us to study four homologous ethyl esters with increasing chain length and one branched isomer (compound **3**). On the one hand, it appears that the vaporization of small ester in aqueous solutions requires a greater amount of energy than the vaporization of pure small esters (ethyl acetate and ethyl butanoate). On the other hand, comparison of ethyl butanoate to its branched isomer ethyl 2-methylpropanoate shows that the consequence of branching results in a lower $\Delta H_{\text{vap}}^{\circ}$ value for pure ethyl 2-methylpropanoate than for pure ethyl acetate and ethyl butanoate and a higher $\Delta H_{\text{eq}}^{\circ}$ value for ethyl 2-methylpropanoate in aqueous solution than for ethyl acetate and ethyl butanoate in aqueous solution. The consequence of branching results also in a decrease of molecule size (RadOfGyration and Jurs-SASA values reported in **Table 6**). For esters having at least a C6 chain, the increase of molecule size leads to an increase in enthalpy variation for pure compounds and to a stagnation and then a decrease (C8 chain) for compounds in aqueous solution (**Figure 3**).

The inset in **Figure 6** displays a zoom on the scatterplot of ΔH° values versus Jurs-FPSA-3 values. Connecting the point allows us to improve visualization and understanding of the relationship between molecular structure and ΔH° values and puts forward the particular behavior of ethyl octanoate, which has the highest Jurs-FPSA-3 value of the ester subset. Therefore, we focused one by one on two subsets: four esters, on the first hand, and five esters, on the second hand.

We obtained an excellent correlation for the five pure esters between $\Delta H_{\text{vap}}^{\circ}$ and PHI (**Table 4**; $r^2 = 0.99$, F test = 224), which confirms the role played by molecular flexibility in the stability of pure liquid phase.

We checked the correlations for $\Delta\Delta H^{\circ}$ values and found a good one with the shape Kappa index Kappa-3-AM (**Table 4**; $r^2 = 0.93$, F test = 43) that satisfactorily explained how the increase in chain length is linked to the difference of enthalpy variation between liquid state and vapor state. Kappa-3-AM is a shape index that encodes the chain length and chain branching considering the counts of paths of length 3; thus, the values increase with the chain length and are greater for nonbranched molecules. This explains the highest $\Delta\Delta H^{\circ}$ value observed for ethyl 2-methyl butanoate and the negative $\Delta\Delta H^{\circ}$ value observed for ethyl octanoate. In the same way, attention is drawn back to the shape viewpoint.

Conversely, for the four esters in aqueous solution we obtained excellent correlations between $\Delta H_{\text{eq}}^{\circ}$ and CHI-V-2 ($r^2 = 0.98$, F test = 78) and Jurs-RPSA ($r^2 = 0.97$, F test = 65), but the correlations obtained with the same descriptors were not so good for the five-ester subset (predicted $\Delta H_{\text{eq}}^{\circ} = 43326 + 2658.64$ CHI-V-2, $r^2 = 0.12$, F test = 0.39; predicted $\Delta H_{\text{eq}}^{\circ} = 61770.7 - 69317.4$ Jurs-RPSA, $r^2 = 0.32$, F test = 1.41), and in this way, ethyl octanoate appeared to be an outlier.

The role of conformation is underscored by the correlation obtained with CHI-V-2 and Jurs-RPSA. Indeed, the correlations are good for the four-ester subset, but bad for the five-ester subset (**Table 4**). CHI-V-2 is a connectivity index that encodes the number of pairs of bonds and thus reflects the chain length and branching and, in this way, some shape characteristics. The calculation of topological indices is based solely on the molecular structure, and their values do not depend on the conformation. CHI-V-2 explains very well the $\Delta H_{\text{eq}}^{\circ}$ enthalpy values of the

C4–C8 chain esters of the subset of four esters and, moreover, takes rightly the branching of ethyl 2-methylpropanoate into account. However, it fails to predict the $\Delta H_{\text{eq}}^{\circ}$ value for ethyl octanoate by simple linear regression.

Additional information was provided by the correlations between $\Delta H_{\text{eq}}^{\circ}$ and Jurs-RPSA. Jurs-RPSA is a surface and electronic spatial descriptor. It encodes the ratio of charged surface area on the molecule, negative as well positive charges. As an electronic descriptor, Jurs-RPSA reflects polar interactions involved between aroma compounds and water, and as a shape- and conformational-dependent descriptor, it gave crucial information. Indeed, it clearly appears that the $\Delta H_{\text{eq}}^{\circ}$ value of ethyl octanoate predicted by Jurs-RPSA is close to enthalpy values determined for ethyl acetate and ethyl butanoate, respectively (**Figure 7**), which means ethyl octanoate in aqueous solution could “mimic” the polarity of a small ester.

Using the correlation observed between $\Delta H_{\text{eq}}^{\circ}$ and Jurs-RPSA for the four-ester subset, we determined the Jurs-RPSA value predicted for ethyl octanoate by the linear equation ($\text{Jurs-RPSA}_{\text{calcd ethyl octanoate}} = 0.2377$). The conformers corresponding to the Jurs-RPSA value of minimized conformer used for alignment and calculated Jurs-RPSA value according to linear regression are displayed in **Figure 8**. Energy, Jurs-SASA, Jurs-TPSA, Jurs-RPSA, and RadOfGyration values are reported in **Table 8**.

Ethyl octanoate-conf1 is the lowest energy conformer and was used for the structure–property study on the whole training set. The chain of octanoate-conf1 (**a**) is extended, the four other conformers (**b–e**) are twisted. Ethyl octanoate-conf2 and ethyl octanoate-conf3 are characterized by Jurs-RPSA values close to the Jurs-RPSA value for ethyl octanoate-conf1 (**Table 8**). Ethyl octanoate-conf4 and ethyl octanoate-conf5 are selected on the basis of linear regression $\Delta H_{\text{eq}}^{\circ}$ versus Jurs-RPSA on the four-ester subset: the predicted Jurs-RPSA value is equal to 0.2377, and Jurs-RPSA values for ethyl octanoate-conf4 and ethyl octanoate-conf5 are, respectively, equal to 0.2360 and 0.2397.

The size of conformers is encoded by RadOfGyration and Jurs-SASA values: the biggest conformer is ethyl octanoate-conf1, whereas the smallest is ethyl octanoate-conf5 (**Table 8**). Ethyl octanoate-conf1 (extended) and ethyl octanoate-conf4 (twisted) have almost the same size. In the same way, ethyl octanoate-conf2 and ethyl octanoate-conf4 present also close sizes. Thus, the surface of ethyl octanoate does not appear as a crucial factor to explain the $\Delta H_{\text{eq}}^{\circ}$ value. The main difference between ethyl octanoate-conf1, -conf2, and -conf3, on the one hand, and ethyl octanoate-conf4 and -conf5, on the other hand, is related to polar surfaces. Indeed, ethyl octanoate-conf4 and ethyl octanoate-conf5 possess the highest values of Jurs-TPSA and Jurs-RPSA, respectively. These values are 1.5 times higher than both Jurs-TPSA values and Jurs-RPSA values of ethyl octanoate-conf1, -conf2, and -conf3.

The common characteristic to ethyl octanoate-conf1, ethyl octanoate-conf2, and ethyl octanoate-conf3 is the orientation of the oxygen atoms of the carboxyl functions on opposite sides of the molecule. Conversely, the oxygen atoms are on the same side for ethyl octanoate-conf4 and ethyl octanoate-conf5, which confers higher Jurs-RPSA values to these conformers.

Our observations suggest that the conformers ethyl octanoate-conf4 and ethyl octanoate-conf5 should be favored conformers in aqueous solution. The role of molecular polarity appears to be more important than the global shape adopted by the conformer to allow the solvation in aqueous solution. We also observed that conformational energies are higher for ethyl octanoate-conf4 and ethyl octanoate-conf5 than for ethyl octanoate-conf1, ethyl octanoate-conf2, and ethyl octanoate-conf3. This energy excess

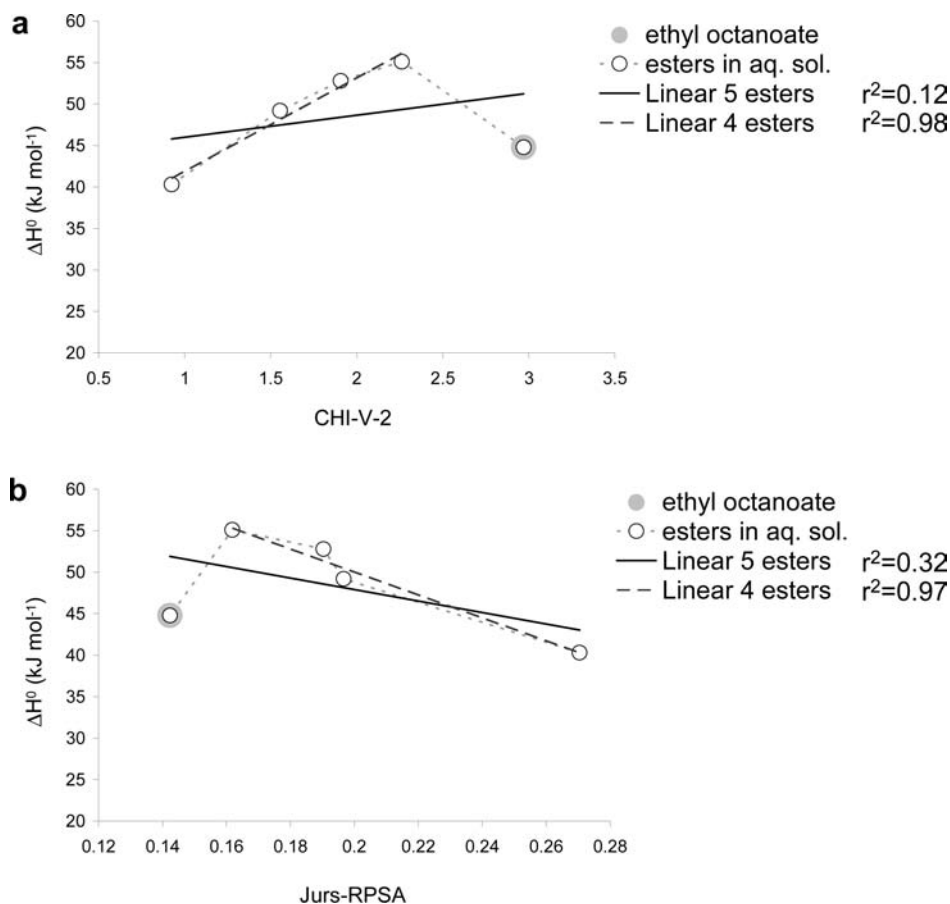


Figure 7. Regression plots of $\Delta H^\circ_{\text{eq}}$ versus CHI-V-2 (a) and of $\Delta H^\circ_{\text{eq}}$ versus Jurs-RPSA (b).

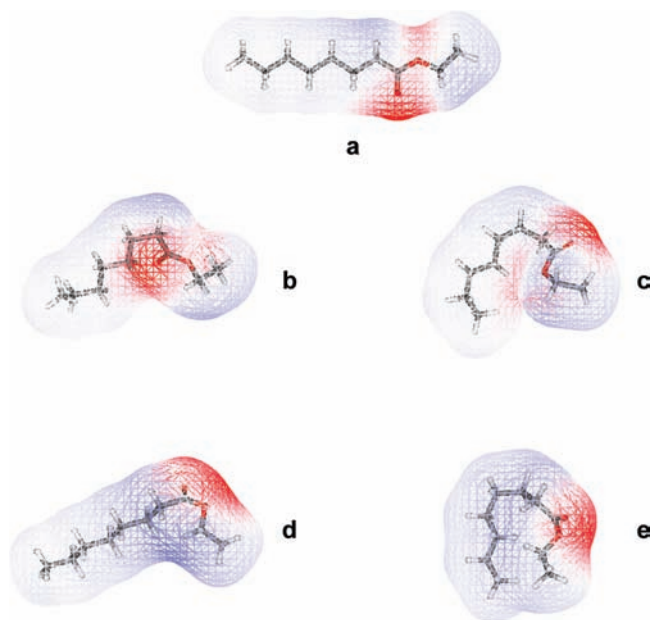


Figure 8. Selected conformers of ethyl octanoate: (a) ethyl octanoate-conf1 used for alignment; ethyl octanoate-conf2 (b) and ethyl octanoate-conf3 (c), Jurs-RPSA values nearest to those of ethyl octanoate-conf1 (a); ethyl octanoate-conf4 (d) and ethyl octanoate-conf5 (e), Jurs-RPSA values predicted by QSAR equation. The van der Waals surfaces are colored according to electrostatic potential values, showing the distribution of charges on the molecule (red for negative charges and blue for positive charge).

Table 8. Energies, Surfaces, and Size Values of Ethyl Octanoate Conformers

conformer	E_{conf} (kcal mol ⁻¹)	RadOf- Gyration (Å)	Jurs- SASA (Å ²)	Jurs- TPSA (Å ²)	Jurs- RPSA
ethyl octanoate-conf1	32.9	4.4	455	69	0.1506
ethyl octanoate-conf2	48.2	3.6	436	62	0.1415
ethyl octanoate-conf3	54.0	3.2	419	61	0.1448
ethyl octanoate-conf4	83.6	3.9	451	106	0.2360
ethyl octanoate-conf5	73.7	2.8	386	93	0.2397

could explain the weak enthalpy value $\Delta H^\circ_{\text{eq}}$ of ethyl octanoate in aqueous solution; insofar that ethyl octanoate-conf4 and ethyl octanoate-conf5 are faintly stable, that makes easier the phase change.

As should be expected, the capacity to involve van der Waals interaction is of major importance for vapor–liquid equilibrium of pure aroma compounds and is illustrated by the correlation of T_{vap} and $\log K_{\text{liq},30^\circ\text{C}}$ with Rotlbonds and PHI, respectively. Conversely, the correlations obtained between thermodynamic equilibrium values (T_{eq} and $\log K_{\text{ret},30^\circ\text{C}}$) and charge descriptors (Jurs-RNCG) put forward the role of polarity in liquid–vapor equilibrium of compounds in aqueous solution. Nevertheless, the difference observed in the values of T and $\log K_{30^\circ\text{C}}$ between pure compounds and compounds in aqueous solution seems to be related to molecule shape, according to the correlation observed

with the connectivity index CHI-V-1. Examination of correlations between T , $\log K_{30^\circ\text{C}}$, ΔH° , and ΔS° , on the one hand, and values of enthalpy and entropy variations, on the other hand, puts forward the key role of enthalpy for vaporization of pure compounds and the key role of entropy in liquid–vapor equilibrium of compounds in aqueous solution. The meaning of vaporization enthalpy values appeared not easy to understand. The role of charged surface areas appeared crucial, but related to the structure of carbon skeleton and also to the twist of conformers. Indeed, in the case of esters, we showed that $\Delta\Delta H^\circ$ variation according to molecular structure is strongly correlated with chain length and branching. On the other hand, examination of ethyl octanoate conformers and related Jurs-RPSA, Jurs-SASA, and conformational energy values suggested that a C10 chain molecule could adopt a relatively high energy conformation that allows its solvation in water. According to the shapes and Jurs-SASA values, it appeared that the decisive factor is the distribution of polar and apolar surfaces on the molecule rather than conformer shape. Nevertheless, the specific orientation of oxygen atoms on the same side of the molecule confers a higher value of polar surface area and appears as a favorable aspect for ester solvation.

Despite its minimalism, our present structure–property relationship approach applied to apparent thermodynamic liquid–vapor equilibrium study leads to improved understanding of the behavior of aroma compounds in aqueous media. Indeed, these equilibria are crucial for aroma compound perception, insofar that aroma compounds are submitted to successive liquid–vapor changes in their transport from the food matrix to the olfactory receptors, through intermediate media such as saliva in the mouth and mucus in the olfactory epithelium. Developing a more sophisticated QSAR study in these media would require consideration in the future of a larger set of aroma compounds, comprising a broad range of structural characteristics such as unsaturation and/or branching.

ABBREVIATIONS AND NOMENCLATURE

C_{liq} , concentration of aroma compounds in liquid phase (mol L^{-1}); C_{vap} , concentration of aroma compounds in vapor phase (mol L^{-1}); V_{vap} , volume of vapor phase (L); V_{liq} , volume of liquid phase (L); p_X , partial pressure of the compound (X) in the vapor phase (atm); PC, partition coefficient expressed as concentration ratio ($\text{PC} = C_{\text{vap}}/C_{\text{liq}}$); \ln , Napierian logarithm; \log , decimal logarithm; K , constant equilibrium ($K = \text{PC} \times RT \times P^\circ/C_0$) shift to vapor phase (K_{exp} , experimental values; K_{calcd} , calculated values according to van't Hoff's equation; R , universal gas constant ($R = 8.314 \text{ J mol}^{-1} \text{ K}^{-1}$; $R = 0.0821 \text{ L atm K}^{-1} \text{ mol}^{-1}$); K_{liq} , constant equilibrium for pure compounds (shift to liquid phase); K_{ret} , constant equilibrium for compounds in aqueous solution (shift to liquid phase); T_{vap} , boiling temperature of pure compounds (K); T_{eq} , liquid–vapor equilibrium temperature of compounds in aqueous solution (change of balance shift) (K); $\Delta H^\circ_{\text{vap}}$, standard vaporization enthalpy of pure compounds (J mol^{-1}); $\Delta H^\circ_{\text{eq}}$, standard vaporization enthalpy of compounds in aqueous solution (J mol^{-1}); $\Delta\Delta H^\circ$, $\Delta\Delta H^\circ = \Delta H^\circ_{\text{eq}} - \Delta H^\circ_{\text{vap}}$ (J mol^{-1}); $\Delta S^\circ_{\text{vap}}$, standard vaporization entropy of pure compounds ($\text{J K}^{-1} \text{ mol}^{-1}$); $\Delta S^\circ_{\text{eq}}$, standard vaporization entropy of compounds in aqueous solution ($\text{J K}^{-1} \text{ mol}^{-1}$); $\Delta\Delta S^\circ$, $\Delta\Delta S^\circ = \Delta S^\circ_{\text{eq}} - \Delta S^\circ_{\text{vap}}$ ($\text{J K}^{-1} \text{ mol}^{-1}$); $\Delta G^\circ_{\text{vap}}$, standard vaporization Gibbs free energy of pure compounds (J mol^{-1}); $\Delta G^\circ_{\text{eq}}$, standard vaporization Gibbs free energy of compounds in aqueous solution (J mol^{-1}); BS- r^2 , bootstrap r^2 ; CV- r^2 , cross-validation r^2 .

LITERATURE CITED

- Guichard, E. Interactions between flavor compounds and food ingredients and their influence on flavor perception. *Food Rev. Int.* **2002**, *18*, 49–70.
- Pelletier, E.; Sostmann, K.; Guichard, E. Measurement of interactions between β -lactoglobulin and flavor compounds (esters, acids, and pyrazines) by affinity and exclusion size chromatography. *J. Agric. Food Chem.* **1998**, *46*, 1506–1509.
- Sostmann, K.; Bernal, B.; Andriot, I.; Guichard, E. Flavour binding by β -lactoglobulin: different approaches. In *Flavor Perception. Aroma Evaluation*; Kruse, H.-P., Rothe, M., Eds.; Eigenverlag Universität Postdam: Eisenach, Germany, 1997; pp 425–434.
- Andriot, I.; Harrison, M.; Fournier, N.; Guichard, E. Interactions between methyl ketones and β -lactoglobulin: sensory analysis, head-space analysis, and mathematical modeling. *J. Agric. Food Chem.* **2000**, *48*, 4246–4251.
- Buttery, R.; Guadagni, D. G.; Ling, L. C. Flavor compounds: volatilities in vegetable oil and oil–water mixtures. Estimation of odor thresholds. *J. Agric. Food Chem.* **1973**, *21*, 198–201.
- Guth, H.; Rusu, M. Food matrices – determination of odorant partition coefficients and application of models for their prediction. *Food Chem.* **2008**, *108*, 1208–1216.
- van Ruth, S. M.; King, C.; Giannouli, P. Influence of lipid fraction, emulsifier fraction, and mean particle diameter of oil-in-water emulsions on the release of 20 aroma compounds. *J. Agric. Food Chem.* **2002**, *50*, 2365–2371.
- Kopjar, M.; Andriot, I.; Saint-Eve, A.; Souchon, I.; Guichard, E. Retention of aroma compounds: an interlaboratory study on the effect of the composition of food matrices on thermodynamic parameters in comparison with water. *J. Sci. Food Agric.* **2010**, in press. DOI 10.1002/jsfa.3929.
- Covarrubias-Cervantes, M.; Mokbel, I.; Champion, D.; Jose, J.; Voilley, A. Saturated vapour pressure of aroma compounds at various temperatures. *Food Chem.* **2004**, *85*, 221–229.
- Reiners, J.; Nicklaus, S.; Guichard, E. Interactions between β -lactoglobulin and flavour compounds of different chemical classes. Impact of the protein on the odour perception of vanillin and eugenol. *Lait* **2000**, *80*, 347–360.
- Dudek, A. Z.; Arodz, T.; Galvez, J. Computational methods in developing quantitative structure–activity relationships (QSAR): a review. *Comb. Chem. High Throughput Screen* **2006**, *9*, 213–228.
- Selassie, C. D. History of quantitative structure–activity relationships. In *Burger's Medicinal Chemistry and Drug Discovery*, 6th ed.; Abraham, D. J., Ed.; Wiley: New York, 2003; Vol. 1: Drug Discovery.
- Todeschini, R.; Consonni, V. *Handbook of Molecular Descriptors – Methods and Principles in Medicinal Chemistry*; Wiley-VCH Verlag: Weinheim, Germany, 2000; Vol. 11, pp 667.
- Chana, A.; Tromelin, A.; Andriot, I.; Guichard, E. Flavor release from *t*-carrageenan matrix: a quantitative structure–property relationships approach. *J. Agric. Food Chem.* **2006**, *54*, 3679–3685.
- Lubbers, S.; Decourcelle, N.; Martinez, D.; Guichard, E.; Tromelin, A. Effect of thickeners on aroma compound behavior in a model dairy gel. *J. Agric. Food Chem.* **2007**, *55*, 4835–4841.
- CANAL-ARLE Project “Conception assistée de nouveaux aliments”. “Interactions Arôme-Aliment-Emballage”, **2003–2005**, INRA.
- Guha, R. On the interpretation and interpretability of quantitative structure–activity relationship models. *J. Comput.-Aided Mol. Des.* **2008**, *22*, 857–871.
- Ettre, L. S.; Kolb, B. Headspace-gas chromatography: the influence of sample volume on analytical results. *Chromatographia* **1991**, *32*, 5–12.
- Brooks, B. R.; Bruccoleri, R. E.; Olafson, B. D.; States, D. J.; Swaminathan, S.; Karplus, M. CHARMM – a program for macromolecular energy, minimization, and dynamics calculations. *J. Comput. Chem.* **1983**, *4*, 187–217.
- Smellie, A.; Teig, S. L.; Tobwin, P. Poling: promoting conformational variation. *J. Comput. Chem.* **1995**, *16*, 171–187.
- Gramatica, P. Principles of QSAR models validation: internal and external. *QSAR Comb. Sci.* **2007**, *26*, 694–701.
- Roy, K. On some aspects of validation of predictive quantitative structure–activity relationship models. *Expert Opin. Drug Discov.* **2007**, *2*, 1567–1577.
- Philippe, E.; Seuvre, A.-M.; Schippa, C.; Voilley, A. Flavour compounds behaviour as a function of temperature in a model emulsion. In *Flavour Research at the Dawn of the Twenty-First*

- Century, 10th Weurman Flavour Research Symposium, Beaune, France; Le Quéré, J. L., Etiévant, P. X., Eds.; Lavoisier – Tec & Doc: Paris, France, 2002; pp 244–247.
- (24) Nongonierma, A. B.; Springett, M.; Le Quéré, J.-L.; Cayot, P.; Voilley, A. Flavour release at gas/matrix interfaces of stirred yoghurt models. *Int. Dairy J.* **2006**, *16*, 102–110.
- (25) Covarrubias-Cervantes, M.; Champion, D.; Debeaufort, F.; Voilley, A. Aroma volatility from aqueous sucrose solutions at low and subzero temperatures. *J. Agric. Food Chem.* **2004**, *52*, 7064–7069.
- (26) Seuvre, A. M.; Turci, C.; Voilley, A. Effect of the temperature on the release of aroma compounds and on the rheological behaviour of model dairy custard. *Food Chem.* **2008**, *108*, 1176–1182.
- (27) Meynier, A.; Garillon, A.; Lethuaut, L.; Genot, C. Partition of five aroma compounds between air and skim milk, anhydrous milk fat or full-fat cream. *Lait* **2003**, *83*, 223–235.
- (28) Frank, H. S.; Evans, M. W. Free volume and entropy in condensed systems III. Entropy in binary liquid mixtures; partial molal entropy in dilute solutions; structure and thermodynamics in aqueous electrolytes. *J. Chem. Phys.* **1945**, *13*, 507.
- (29) Ashbaugh, H. S.; Truskett, T. M.; Debenedetti, P. G. A simple molecular thermodynamic theory of hydrophobic hydration. *J. Chem. Phys.* **2002**, *116*, 2907–2921.
- (30) Ben-Amotz, D. Global thermodynamics of hydrophobic cavitation, dewetting, and hydration. *J. Chem. Phys.* **2005**, *123*, 8–15.
- (31) Blokzijl, W.; Engberts, J. Hydrophobic effects – opinions and facts. *Angew. Chem.–Int. Ed. Engl.* **1993**, *32*, 1545–1579.
- (32) Lazaridis, T. Solvent size vs cohesive energy as the origin of hydrophobicity. *Acc. Chem. Res.* **2001**, *34*, 931–937.
- (33) Muller, N. Search for a realistic view of hydrophobic effects. *Acc. Chem. Res.* **1990**, *23*, 23–28.
- (34) Shinoda, K.; Fujihira, M. The analysis of the solubility of hydrocarbons in water. *Bull. Chem. Soc. Jpn.* **1968**, *41*, 2612–2615.
- (35) Southall, N. T.; Dill, K. A.; Haymet, A. D. J. A view of the hydrophobic effect. *J. Phys. Chem. B* **2002**, *106*, 521–533.
- (36) Dunitz, J. D. Win some, lose some – enthalpy–entropy compensation in weak intermolecular interactions. *Chem. Biol.* **1995**, *2*, 709–712.
- (37) Guha, R.; Dutta, D.; Jurs, P. C.; Chen, T. Local lazy regression: making use of the neighborhood to improve QSAR predictions. *J. Chem. Inf. Model.* **2006**, *46*, 1836–1847.
- (38) Guha, R.; Jurs, P. C. Determining the validity of a QSAR model – a classification approach. *J. Chem. Inf. Model.* **2005**, *45*, 65–73.
- (39) Weaver, S.; Gleeson, N. P. The importance of the domain of applicability in QSAR modeling. *J. Mol. Graph.* **2008**, *26*, 1315–1326.
- (40) Hall, L. H.; Kier, L. B.; Murray, C. W. Molecular connectivity. 2: Relationship to water solubility and boiling point. *J. Pharm. Sci.* **1975**, *64*, 1974–1977.
- (41) Katritzky, A. R.; Slavov, S. H.; Dobchev, D. A.; Karelson, M. Rapid QSPR model development technique for prediction of vapor pressure of organic compounds. *Comput. Chem. Eng.* **2007**, *31*, 1123–1130.
- (42) Stanton, D. T.; Jurs, P. C. Development and use of charged partial surface area structural descriptors in computer-assisted quantitative structure–property relationship studies. *Anal. Chem.* **1990**, *62*, 2323–2329.
- (43) Singh, J.; Singh, S.; Shaik, B.; Deeb, O.; Sohani, N.; Agrawal, V. K.; Khadikar, P. V. Mutagenicity of nitrated polycyclic aromatic hydrocarbons: a QSAR investigation. *Chem. Biol. Drug Design* **2008**, *71*, 230–243.
- (44) Randić, M. The connectivity index 25 years after. *J. Mol. Graph.* **2001**, *20*, 19–35.
- (45) David, V.; Medvedovici, A. Structure–retention correlation in liquid chromatography for pharmaceutical applications. *J. Liq. Chromatogr. Relat. Technol.* **2007**, *30*, 761–789.
- (46) Majer, V.; Svoboda, V.; Pechacek, J.; Hala, S. Enthalpies of vaporization and cohesive energies of eight c-9 to c-11 alkanes. *J. Chem. Thermodyn.* **1984**, *16*, 567–572.
- (47) Li, L. N.; Xie, S. D.; Cai, H.; Bai, X. T.; Xue, Z. Quantitative structure–property relationships for octanol–water partition coefficients of polybrominated diphenyl ethers. *Chemosphere* **2008**, *72*, 1602–1606.
- (48) Murray, J. S.; Abu-Awwad, F.; Politzer, P. Prediction of aqueous solvation free energies from properties of solute molecular surface electrostatic potentials. *J. Phys. Chem. A* **1999**, *103*, 1853–1856.
- (49) Baudot, A.; Souchon, I.; Marin, M. Total permeate pressure influence on the selectivity of the pervaporation of aroma compounds. *J. Membr. Sci.* **1999**, *158*, 167–185.
- (50) Carelli, A. A.; Crapiste, G. H.; Lozano, J. E. Activity coefficients of aroma compounds in model solutions simulating apple juice. *J. Agric. Food Chem.* **1991**, *39*, 1636–1640.
- (51) Druaux, C.; Le Than, M.; Seuvre, A. M.; Voilley, A. Application of headspace analysis to the study of aroma compounds–lipids interaction. *J. Am. Oil Chem. Soc.* **1998**, *75*, 127–130.
- (52) Fares, K.; Landy, P.; Guillard, R.; Voilley, A. Physicochemical interactions between aroma compounds and milk proteins: effect of water and protein modification. *J. Dairy Sci.* **1998**, *81*, 82–91.
- (53) Harvey, B. A.; Druaux, C.; Voilley, A. Effect of protein on the retention and transfer of aroma compounds at the lipid–water interface. In *Food Macromolecule and Colloids*; Lorient, E. D. a. D., Ed.; The Royal Society of Chemistry: London, U.K., 1995; pp 154–163.
- (54) Kolb, B.; Welter, C.; Bichler, C. Determination of partition coefficients by automatic equilibrium headspace gas chromatography by vapor phase calibration. *Chromatographia* **1992**, *34*, 235–240.
- (55) Landy, P.; Druaux, C.; Voilley, A. Retention of aroma compounds by proteins in aqueous solution. *Food Chem.* **1995**, *54*, 387–392.
- (56) Landy, P.; Fares, K.; Lorient, D.; Voilley, A. Effect of chemical modification of sodium caseinate on diffusivity of aroma compounds in aqueous solutions. *J. Agric. Food Chem.* **1997**, *45*, 2649–2653.
- (57) Le Thanh, M. Extraction de substances aromatisantes produites par voie microbiologique. Doctoral Thesis, Université de Bourgogne, Dijon, France, **1992**.
- (58) Le Thanh, M.; Lamer, T.; Voilley, A.; Jose, J. Détermination des coefficients de partage vapeur-liquide et d'activité de composés d'arôme à partir de leurs caractéristiques physico-chimiques. *J. Chim. Phys.* **1993**, *90*, 545–60.
- (59) Le Thanh, M.; Pham, S. T.; Voilley, A. Influence de la présence d'huile végétale en émulsion sur la volatilité de substances aromatisantes au cours de l'extraction. *Sci. Aliment.* **1992**, *12*, 587–592.
- (60) Le Thanh, M.; Thibeau, P.; Thibaut, M. A.; Voilley, A. Interactions between volatile and non-volatile compounds in the presence of water. *Food Chem.* **1992**, *43*, 129–135.
- (61) Le Thanh, M.; Voilley, A.; Phan Tan Luu, R. Influence de la composition d'un milieu de culture modèle sur le coefficient de partage vapeur-liquide de substances aromatisantes. *Sci. Aliment.* **1993**, *699*–710.
- (62) Marinos, D.; Saravacos, G. *Volatility of Organic Compounds in Aqueous Sucrose Solutions*, 5th International Congress of Chemical and Process Engineering CHISA, Prague, Czech Republic, 1975.
- (63) Nelson, P. E.; Hoff, J. E. Food volatiles: gas chromatographic determination of partition coefficients in water–lipid systems. *J. Food Sci.* **1968**, *33*, 479–482.
- (64) Pividal, K. A.; Birtigh, A.; Sandler, S. I. Infinite dilution activity coefficients for oxygenate systems determined using a differential static cell. *J. Chem. Eng. Data* **1992**, *37*, 484–487.
- (65) Sancho, M. F.; Rao, M. A.; Downing, D. L. Infinite dilution activity coefficients of apple juice aroma compounds. *J. Food Eng.* **1997**, *34*, 145–158.
- (66) Sorrentino, F.; Voilley, A.; Richon, D. Activity coefficients of aroma compounds in model food systems. *AIChE J.* **1986**, *32*, 1988–1993.
- (67) Voilley, A.; Bosset, J. O. Nouvelle technique de détermination rapide de la volatilité de composés d'arôme dans les milieux à forte viscosité. *Lebensm. Wiss. Technol.* **1986**, *19*, 47–52.
- (68) Voilley, A.; Sauvageot, F. Effet du saccharose sur l'intensité de l'odeur de deux substances d'arôme en solution aqueuse. *Sci. Aliment.* **1987**, *7*, 59–64.
- (69) Jouquand, C.; Ducruet, V.; Giampaoli, P. Partition coefficients of aroma compounds in polysaccharide solutions by the phase ratio variation method. *Food Chem.* **2004**, *85*, 467–474.
- (70) Landy, P.; Courthaudon, J.-L.; Dubois, C.; Voilley, A. Effect of interface in model food emulsions on the volatility of aroma compounds. *J. Agric. Food Chem.* **1996**, *44*, 526–530.

- (71) Stanford, M. A.; McGorin, J. Flavor volatilization in microwave food model systems. In *Thermally Generated Flavors*; Parliment, T. H., Morello, M. J., McGorin, R. J., Eds.; American Chemical Society: Washington, DC, 1994.
- (72) van Ruth, S. M.; Villeneuve, E. Influence of β -lactoglobulin, pH and presence of other aroma compounds on the air/liquid partition coefficients of 20 aroma compounds varying in functional group and chain length. *Food Chem.* **2002**, *79*, 157–164.
- (73) Gierczynski, I.; Labouré, H.; Sémon, E.; Guichard, E. Impact of hardness of model fresh cheese on aroma release: in vivo and in vitro study. *J. Agric. Food Chem.* **2007**, *55*, 3066–3073.
- (74) Hirata, Y.; Massey, M.; Relkin, P.; Nunes, P.; Ducruet, V. Influence of proteins on the release of aroma compounds into polymer film. *Dev. Food Sci.* **2006**, *43*, 473–476.
- (75) Jouenne, E. Etude des interactions entre la β -lactoglobuline et les composés d'arôme. Doctoral Thesis, Montpellier 2, Montpellier, France, **1997**.
- (76) Landy, P.; Rogacheva, S.; Lorient, D.; Voilley, A. Thermodynamic and kinetic aspects of the transport of small molecules in dispersed systems. *Colloids Surf. B* **1998**, *12*, 57–65.
- (77) Langourieux, S.; Crouzet, J. Study of aroma compounds–polysaccharides interactions by dynamic exponential dilution. *Lebensm. Wiss. Technol.* **1994**, *27*, 544–549.
- (78) Lubbers, S. Caractérisation de macromolécules d'origine levurienne du vin. Etude des interactions avec des substances d'arôme. Application à la stabilité tartrique. Doctoral Thesis, Université de Bourgogne, Dijon, France, **1993**.
- (79) Savary, G.; Guichard, E.; Doublier, J. L.; Cayot, N. Mixture of aroma compounds: determination of partition coefficients in complex semi-solid matrices. *Food Res. Int.* **2006**, *39*, 372–379.
- (80) Voilley, A.; Lubbers, S. Flavor-matrix interactions in wine. Presented at the 213th ACS National Meeting, San Francisco, CA, **1998**.
- (81) Bylaite, E.; Ilgunaite, Z.; Meyer, A. S.; Adler-Nissen, J. Influence of λ -carrageenan on the release of systematic series of volatile flavor compounds from viscous food model systems. *J. Agric. Food Chem.* **2004**, *52*, 3542–3549.
- (82) Buttery, R. G.; Ling, L. C.; Guadagni, D. G. Volatilities of aldehydes, ketones, and esters in dilute water solution. *J. Agric. Food Chem.* **1969**, *17*, 385–389.
- (83) Jouenne, E.; Crouzet, J. Interactions of β -lactoglobulin with flavour compounds. In *Flavour Science. Recent Developments*; Taylor, A. J., Mottram, D. S., Eds.; The Royal Society of Chemistry: Chambruge, U.K., 1996; pp 425–429.
- (84) Nawar, W. W. Some variables affecting composition of headspace aroma. *J. Agric. Food Chem.* **1971**, *19*, 1057–1059.
- (85) Hall, G.; Andersson, J. Volatile fat oxidation-products. 2. Influence of temperature on volatility of saturated, mono-unsaturated and di-unsaturated aldehydes in liquid-media. *Lebensm.–Wiss. Technol.* **1983**, *16*, 362–366.
- (86) Sadafian, A.; Crouzet, J. Infinite dilution activity coefficients and relative volatilities of some aroma compounds. *Flavour Fragrance J.* **1987**, *2*, 103–107.
- (87) Amore, J. E.; Buttery, R. G. Partition-coefficients and comparative olfactometry. *Chem. Senses Flavor* **1978**, *3*, 57–71.
- (88) Burnett, M. G. Determination of partition coefficients at infinite dilution by the gas chromatographic analysis of the vapor above dilute solutions. *Anal. Chem.* **2002**, *35*, 1567–1570.
- (89) Chung, S.; Villota, R. Binding of alcohols by soy protein in aqueous solutions. *J. Food Sci.* **1989**, *54*, 1604–1606.
- (90) Lebert, A.; Richon, D. Study of the influence of solute (*n*-alcohols and *n*-alkanes) chain length on their retention by purified olive oil. *J. Food Sci.* **1984**, *49*, 1301–1304.
- (91) Li, J.; Carr, P. W. Measurement of water–hexadecane partition coefficients by headspace gas chromatography and calculation of limiting activity coefficients in water. *Anal. Chem.* **1993**, *65*, 1443–1450.
- (92) Randić, M. On characterization of molecular branching. *J. Am. Chem. Soc.* **1975**, *97*, 6609–6615.

Received for review July 16, 2009. Revised manuscript received February 19, 2010. Accepted February 22, 2010. This work was supported by a grant provided by the Conseil Régional de Bourgogne (France) to M.K.